"IMPLEMENTATION OF THE PROPOSED DPOAE ESTIMATION TECHNIQUE"

The Thesis submitted in partial fulfillment of the requirements for the award of the degree of

MASTER OF ENGINEERING
IN
ELECTRONICS AND COMMUNICATION ENGINEERING

Submitted By:

HARPREET SINGH RAHIL
Regn. No-8044111

Under the guidance of

Mr. BALWANT SINGH
SENIOR LECTURER, ECED
(TIET, PATIALA)

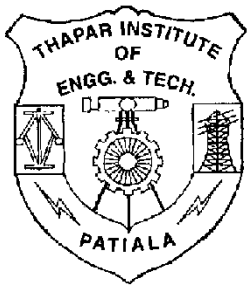

DEPARTMENT OF ELECTRONICS AND COMMUNICATION ENGINEERING

THAPAR INSTITUTE OF ENGINEERING & TECHNOLOGY
(DEEMED UNIVERSITY),
PATIALA – 147004.

YEAR 2006

CERTIFICATE

I, HARPREET SINGH RAHIL hereby certify that the work which is being presented in this thesis entitled **"IMPLEMENTATION OF THE PROPOSED DPOAE ESTIMATION TECHNIQUE"** by me in partial fulfillment of requirements for the award of degree of Master of Engineering in Electronics and Communication from THAPAR INSTITUTE OF ENGG. & TECH.(Deemed University), PATIALA, is an authentic record of my own work carried under the supervision of Mr. BALWANT SINGH at TIET, PATIALA.

The matter presented in this thesis has not been submitted in any other University or Institute for the award of any degree.

(**HARPREET SINGH RAHIL**)
Signature of the student
8044111

This is certified that the above statement made by the candidate is correct to the best of my knowledge.

(Mr. BALWANT SINGH)
SENIOR LECTURER, TIET PATIALA
GUIDE

Head of Department, ECED
T.I.E.T., PATIALA.

Dean of Academic Affairs,
T.I.E.T., PATIALA.

ACKNOWLEGEMENT

Words are often too less to reveal one's deep regards. An understanding of the work like this is never the outcome of the efforts of a single person. I take this opportunity to express my profound sense of gratitude and respect to all those who helped me through the duration of this thesis.

First, I would like to thank the Supreme Power, the GOD, who guided me to work on the right path of life. Without his grace, this would not have been possible. This work would not have been possible without the encouragement and able guidance of **'Mr. BALWANT SINGH'**, Senior Lecturer, TIET, PATIALA. Their enthusiasm and optimism made this experience both rewarding and enjoyable. Most of the novel ideas and solutions found in this thesis are the result of our numerous stimulating discussions. His feedback and editorial comments were also invaluable for the writing of this thesis. I am grateful to **Head of the Department Dr. R. S. KALER** and **Dr. A.K. CHATTERJEE, PG Coordinator** for providing the facilities for the completion of thesis.

I take pride of my self being son of ideal great parents whose everlasting desire, sacrifice, affectionate blessing and help without which it would have not been possible for me to complete my studies.

At last, I would like to thank all the members and employees of Electronics and Communication Department, TIET Patiala whose love and affection made this possible.

(HARPREET SINGH RAHIL)

ABSTRACT

Implementation of the proposed DPOAE estimation technique is presented A new method of measurement of distortion product otoacoustic emission (DPOAE) signal level based on a recently introduced nonlinear adaptive method of extraction of non-stationary sinusoids is presented. Performance of the proposed method is demonstrated with the aid of computer simulations. Comparison is made between the proposed technique and existing methods. The proposed method features structural simplicity which renders it particularly attractive for implementation on software (MATLAB). It offers a high degree of immunity with regard to background noise and parameter variations. Compared to conventional methods, the proposed method offers a shorter measurement time which is of significant value. The purpose of developing this technique is to improve on already existing methods in the amount of time required for a subject to undergo the test, as well as the need for sound-proof environments. The basis of this technique is an algorithm, which is effective in extracting sinusoids from noise. The algorithm is found to be extremely robust with respect to both changes in internal parameters and fluctuations in external conditions. Combining this algorithm with some supportive signal processing modules, such as band-pass filters, allows for a quick and effective means to test the auditory response by attempting to extract a low-level sinusoid known as the distortion product otoacoustic emission (DPOAE). The development of the real-time application begins with digitizing and codifying the continuous model in the MATLAB environment. It is observed that this method of DPOAE estimation outperforms other linear estimation techniques, including the discrete Fourier transform (DFT). It offers a high degree of noise immunity while providing relatively faster measurements.

TABLE OF CONTENTS

CHAPTER TITLE **PAGE No.**

Certificate ……....i

Acknowledgement……....ii

Abstract……....iii

Table of Contents……....iv

List of Figures…….....vii

List of Tables……xi

Chapter 1 Introduction

1.1 Introduction……1

1.2 Review of Hearing Assessment Methods ……..2

1.2.1 Overview……..2

1.2.1.1 Spontaneous Otoacoustic Emissions…….3

1.2.1.2 Transient Evoked Otoacoustic Emissions…….3

1.2.1.3 Distortion Product Otoacoustic Emissions…….....3

1.2.2 Existing DPOAE Estimation Methods…….4

1.3 Outline of the Thesis….....6

Chapter 2 DFT And DSP Implementation

2.1 Introduction ……...……7

2.2 Core Algorithm Implementation……9

Chapter 3 DPOAE Estimation Method And Implementation

3.1 Introduction……...11

CHAPTER TITLE PAGE No.

3.2 Structure of a DPOAE measurement device……12
3.3 Proposed Technique……..13
3.3.1 Core Algorithm Implementation……16
3.3.2 Variation of Parameters……19
3.4 Simulation…….....20
3.5 Filter Design…….....24
3.6 Time-Gating……..28
3.7 Input Signal Generation……29

Chapter 4 Simulation Results

4.1 Simulation Results…….30
4.2 Results for Input Signal……..33
4.3 Results for Frequency Content of Input Signal……...34
4.4 Results for output of pre-processing BPF……...36
4.5 Results for frequency content output of pre-processing BPF…….37
4.6 Results for output of artifact removal…….39
4.7 Results for frequency content of output of artifact removal……...40
4.8 Results for the output of mid-processing BPF……42
4.9 Results for the frequency content of the output from mid-processing BPF……43
4.10 Results for the output of DPOAE extraction…….45
4.11 Results for the frequency content of output after DPOAE extraction……...46
4.12 Results for DPOAE after post-processing ……48
4.13 Results for the frequency content DPOAE after post-processing…….49
4.14 Results for the DPOAE level after post-processing ……51

CHAPTER	TITLE	PAGE No.

Chapter 5 Conclusion and Future Scope……54

References...…….....55

List of Publications……....58

LIST OF FIGURES

RE No.	NAME OF FIGURE	PAGE No.
2.1	Nyquist Interval	8
3.1	Block diagram of a DPOAE measurement device	12
3.2	Details of a data acquisition system and probe units	12
3.3	Block diagram of the original DPOAE estimation method	15
3.4	Block diagram representation of the employed core algorithm	18
3.5	The performance of the discrete core algorithm in Matlab with $\mu_1 = \mu_2 = 200$	22
3.6	The performance of the discrete core algorithm in Matlab with $\mu_1 = \mu_2 = 20$	23
4.1	Illustration of a 16, 32 and 128-point DFT by using Hamming Window	31
4.2	Illustration of a 16, 32 and 128 point DFT by using Rectangular Window	32
4.3	Illustration of a magnified view of the input signal with a low noise floor with f_1=1000Hz	33
4.4	Illustration of a magnified view of the input signal with a low noise floor with f_1=2000Hz	33
4.5	Illustration of a magnified view of the input signal with a low noise floor with f_1=3000Hz	34
4.6	Illustration of a frequency content of the input signal with f_1=1000Hz	34

RE No.	NAME OF FIGURE	PAGE No.
4.7	Illustration of a frequency content of the input signal with f_1=2000Hz	35
4.8	Illustration of a frequency content of the input signal with f_1=3000Hz	35
4.9	Illustration of the output of pre-processing BPF with f_1=1000Hz	36
4.10	Illustration of the output of pre-processing BPF with f_1=2000Hz	36
4.11	Illustration of the output of pre-processing BPF with f_1=3000Hz	37
4.12	Illustration of a frequency content of the output from pre-processing BPF with f_1=1000Hz	37
4.13	Illustration of a frequency content of the output from pre-processing BPF with f_1=2000Hz	38
4.14	Illustration of a frequency content of the output from pre-processing BPF with f_1=3000Hz	38
4.15	Illustration of the output of artifact removal with f_1=1000Hz	39
4.16	Illustration of the output of artifact removal with f_1=2000Hz	39
4.17	Illustration of the output of artifact removal with f_1=3000Hz	40
4.18	Illustration of the frequency content of output of artifact removal with f_1=1000Hz	40
4.19	Illustration of the frequency content of output of artifact removal with f_1=2000Hz	41

RE No.	NAME OF FIGURE	PAGE No.
4.20	Illustration of the frequency content of output of artifact removal with f_1=3000Hz	41
4.21	Illustration of the output of mid-processing BPF with f_1=1000Hz	42
4.22	Illustration of the output of mid-processing BPF with f_1=2000Hz	42
4.23	Illustration of the output of mid-processing BPF with f_1=3000Hz	43
4.24	Illustration of a frequency content of the output from mid-processing BPF with f_1=1000Hz	43
4.25	Illustration of a frequency content of the output from mid-processing BPF with f_1=2000Hz	44
4.26	Illustration of a frequency content of the output from mid-processing BPF with f_1=3000Hz	44
4.27	Illustration of the output of DPOAE extraction with f_1=1000Hz	45
4.28	Illustration of the output of DPOAE extraction with f_1=2000Hz	45
4.29	Illustration of the output of DPOAE extraction with f_1=3000Hz	46
4.30	Illustration of the frequency content of output after DPOAE extraction with f_1=1000Hz	46
4.31	Illustration of the frequency content of output after DPOAE extraction with f_1=2000Hz	47
4.32	Illustration of the frequency content of output after DPOAE extraction with f_1=3000Hz	47

JRE No.	NAME OF FIGURE	PAGE No.
4.33	Illustration of the DPOAE after post-processing with f_1=1000Hz	48
4.34	Illustration of the DPOAE after post-processing with f_1=2000Hz	48
4.35	Illustration of the DPOAE after post-processing with f_1=3000Hz	49
4.36	Illustration of the frequency content of DPOAE after post processing with f_1=1000Hz	49
4.37	Illustration of the frequency content of DPOAE after post processing with f_1=2000Hz	50
4.38	Illustration of the frequency content of DPOAE after post processing with f_1=3000Hz	50
4.39	Illustration of the DPOAE level after post-processing with f_1=1000Hz	51
4.40	Illustration of the DPOAE level after post-processing with f_1=2000Hz	51
4.41	Illustration of the DPOAE level after post-processing with f_1=3000Hz	52

LIST OF TABLES

LE No.	NAME OF TABLE	PAGE No.
4.1	Frequency Change And Random Constant Phases	52
4.2	Frequency Change And Constant Random Phase	52

CHAPTER 1

INTRODUCTION

1.1 Introduction

Distortion product otoacoustic emissions (DPOAEs) are very low level stimulated acoustic responses to two pure tones presented to the ear canal. DPOAE measurement provides an objective noninvasive measure of peripheral auditory function and is used for hearing assessment especially in newborns [1]. DPOAEs have been recognized for a number of years [2], [3]. However, DPOAE measurement is considered an active area of research because of the challenging nature of the signal processing task.

In this type of otoacoustic test, two pure tones with frequencies f_1 and f_2 are presented to the cochlea. For best results, f_2 is usually chosen as $1.2\,f_1$. Since the ear is a nonlinear structure, a number of very low level distortion products are generated due to the intermodulation process within the cochlea. Among various distortion products, the component with frequency $f_d = 2f_1 - f_2$ is usually the strongest. The level of such a distortion product (commonly referred to as the DPOAE signal) is taken as an index of the functionality of the ear. Estimation of such a weaksignal buried under two strong stimuli and other intermodulations in a potentially noisy background is a challenging signal processing problem.

Conventionally, the discrete Fourier transform (DFT) has been used as the main signal processing tool to estimate the level of the DPOAE signals. Application of the DFT to this problem has a number of shortcomings, among which the long measurement time is the most pronounced one [4]. Long measurement time is usually required for the acquisition of a sufficiently large amount of data which, when averaged, will reduce the overall background noise effect. In addition to the need to increase the measurement time, the tests are usually required to be conducted in low noise environments such as sound-proof rooms or other types of sound-proof enclosures.

There are many ways to test the human auditory response. Some methods are quite primitive, involving tuning forks, while others use state of the art electronics and computers to track nerve signals. The traditional techniques often require a behavioral response. However, some groups of the human population cannot give a behavioral response, the largest being infants. Severe developmental repercussions can occur if an infant is not diagnosed as hearing impaired. Treatment for abnormal hearing needs to begin before six months of age. This time of a child's life is one of the most important periods for speech and language development, which is directly tied with his or her ability to hear. Therefore, the development of a technique to perform auditory testing on infants has a high priority.

This thesis presents the implementation of a hearing testing technique. The technique is based on a recently introduced method of estimation of a distortion product otoacoustic emission (DPOAE) [4]. The proposed technique is centered around a robust nonlinear adaptive signal processing algorithm presented in [6],[7] and attempts to improve on the shortcomings of previous method used.

1.2 Review of Hearing Assessment Methods

1.2.1 Overview

Otoacoustic emissions were first discovered in 1978 and presented in [8],[9].Estimation of otoacoustic emissions (OAEs) is produced by the outer hair cell (OHCs) of normal cochleas, either spontaneously or in response to stimuli in the form of sound [5]. If an OAE is present in the absence of any stimulus, it is referred to as a spontaneous otoacoustic emission (SOAE). OAEs that result from stimuli are known as evoked otoacoustic emissions (EOAEs). Two types of EOAEs are used for hearing assessment: transient evoked otoacoustic emissions (TEOAEs) and distortion product ototacoustic emissions (DPOAEs).The ability of an EOAE to signify normal hearing without behavioral feedback from the patient, along with its noninvasive measurement procedure allow it to become the basis for most neonatal hearing screening [8].

1.2.1.1 Spontaneous Otoacoustic Emissions

SOAEs are low-level narrow band signals produced in the cochlea. They appear to have a correlation with other types of OAEs and are believed to be linked to higher auditory sensitivity [10]. However, their absence does not indicate a loss of hearing in the patient [10]. The inability for a person with normal hearing to produce SOAEs, combined with other aspects such as their strong gender-prevalence (more prevalent in women than men) and asymmetry (stronger and more numerous in the right ear) [12], make this type of OAE an unlikely candidate for the development of a hearing assessment method.

1.2.1.2 Transient Evoked Otoacoustic Emissions

TEOAEs are produced by a subjecting the ear canal to a click. This type of EOAE is present in normal ears, indicating normality in the cochlea [13], which makes it a possible choice for hearing assessment. Although TEOAEs can determine functionality of the inner ear, there are some drawbacks. One drawback is the inability for this method to test for hearing loss at higher frequencies. TEOAEs become unreliable around 5 kHz [5]. Another drawback involves the inability of TEOAEs to perform hearing assessment evaluation at specific frequencies, since TEOAEs are often missing in narrow bands of normal ears [5].

1.2.1.3 Distortion Product Otoacoustic Emissions

Unlike TEOAEs, DPOAEs are believed to be produced by an active nonlinear process located in the cochlea. Since the presence of DPOAEs signifies the presence of this nonlinear cochlear process, it is believed that they can be used to effectively diagnose dysfunctions of sound processing in the inner ear [25]. DPOAE estimation is used to determine the extent of hearing impairment and sudden hearing loss (SHL). A noise damaged cochlea may still produce DPOAEs. However, due to the noise damage, which causes a loss of OHCs, and in turn a linearization of cochlear function, a decrease in DPOAE amplitude will occur [11], [23, [24]. The amplitude of a DPOAE is strongly correlated with the hearing threshold [25]. Therefore, not only the presence of a DPOAE, but also comparing its amplitude to an established set of norms is used to determine

sensorineural hearing impairments [14], [15]. Since a DPOAE is an EOAE, the ear and in turn the cochlea must be subjected to stimuli. In the case of DPOAEs, the stimuli consist of two pure tones, known as primaries, in the audible range. However, the primaries must be close enough in frequency in order to react nonlinearly . If the first tone is located at frequency f_1 and the second at f_2, and f_1 and f_2 are relatively close (within several hundred hertz), the distortion products (DPs) will occur at $n f_1 + mf2$ frequencies, where n and m are integers [25]. Although many DPs are produced, the DP located at $f_d = 2 f_1 - f_2$, which is known as the cubic DP, will always be the largest in terms of amplitude [1, 5, 16, 25]. In addition to being the largest, the cubic DP, is also the most robust [1]. It is observed remaining constant over several minutes of measurement during experimentation, while other DPs vary with time . The frequency ratio also has an impact on the DPs. In order to maximize the cubic DP, research has indicated that $f_2 = f_1$ should equal 1.2 [5]. From this point on the cubic DP will be referred to as the DPOAE.

Although any two primaries in the audible range with a frequency ratio $f_2 = f_1 = 1.2$ and sufficient sound pressure level (SPL) will produce a DPOAE, there are considerations that should be taken into account. The primary consideration should be age group. Different age groups respond differently to different frequency ranges of the primaries [3]. The other factor to be taken into account is the level of the primaries in terms of SPL in decibels (dB). Since the DPOAE level is dependant on the level of the primary, it is desired to choose a primary level high enough to make the DPOAE easy to estimate.

1.2.2 Existing DPOAE Estimation Methods

DPOAE estimation tests are performed much like other methods of EOAEs. A speaker or speakers subject the ear canal to the primaries. A microphone placed within the ear canal records the sound present there. The difficulty in DPOAE estimation is isolating the low level DPOAE from the surrounding noise, which includes the high level primaries. Current methods must be employed in low noise environments such as sound proof-rooms [4]. This makes clinical application of DPOAE measurement somewhat

burdensome. Also, the infant must lie still and refrain from making internal noises, such as swallowing [5].

Many works in the area of DPOAE signal estimation involve adaptive noise cancellation (ANC) [5],[22] and adaptive Wiener filtering (AWF). In each of these techniques, the goal is to improve the signal to noise ratio (SNR) by reducing the noise floor. A reference signal, usually a recording from an auxiliary microphone placed in the ear not under examination, provides a stochastic measure of the background noise [4]. The data from this microphone is used to mitigate the noise recorded by the microphone in the ear under examination. In all these techniques, an estimator is required to approximate the DPOAE signal level. In most cases the estimators are discrete Fourier transform (DFT) based. DFT estimators pose serious shortcomings, the primary being long measurement time in order to provide sufficient resolution and accuracy [4]. Even with this attempt at the reduction of the noise floor, the need for a sound-proof or low noise environment is still essential to reduce testing time by a significant amount. In addition to this restrictive type of environment, high performance computational resources are usually necessary, adding to the overall cost. Therefore, although improvements over the DFT are observed in each case, neither is commonly used in clinical applications.

Other problems inherent in the DFT are its window-based nature and its sensitivity with regard to frequency. A technique employed in an attempt to obviate these shortcomings is presented in [20],[24]. This approach is known as a maximum-likelihood estimator (MLE), although it does provide a superior performance to DFT by increasing the accuracy while decreasing the testing time [19],[21], the MLE technique still suffers from a sensitivity to background noise and internal parameter variations [4]. Therefore, MLEs are not an optimal choice for DPOAE estimation.

In essence, the existing methods of DPOAE estimation fail to provide a robust clinical application. The majorities are DFT-based, and therefore are susceptible to its inherent flaws. Other techniques may provide improvements, but they still suffer from their lack of noise immunity or algorithm complexity.

1.3 Outline of the Thesis

- This thesis begins with a brief introduction to Distortion product otoacoustic emissions (DPOAEs) with a general background on hearing assessment methods.
- Chapter 2 gives a brief introduction to DFT and Real-Time DSP Implementation. This section describes the system hardware performing the estimation process and the development of the controlling software, or firmware, of the DSP.
- Chapter 3 gives a brief introduction to the employed method of DPOAE estimation. The method of DPOAE estimation that is developed into a real-time DSP application is presented in [4] and discussed in this chapter
- Chapter 4 describes the DSP Implementation, This chapter discusses the considerations and procedure of implementing the DPOAE estimation method.
- Chapter 5 gives the simulation results of the implementation of the Distortion product otoacoustic emissions (DPOAEs), along with a comparison to DFT.
- Chapter 6 gives the conclusion and future scope of the work proposed in this thesis .

CHAPTER 2

DFT AND DSP IMPLEMENTATION

2.1 Introduction

This chapter describes the DFT (Discrete Fourier Transform) & DSP implementation of the algorithm. The DFT is an extremely important tool in the digital processing of discrete-time signals by discrete-time systems. The DFT is a discrete-frequency representation of finite-duration sequences and, as a consequence, it becomes a powerful tool in the digital processing of discrete-time signals. The Fourier Transform shown (2.1) transforms a continuous-time function x(t) into a continuous-frequency function X(ω). The same equation can also be written in terms of frequency f instead of angular velocity ω; this version is shown in (2.2). A continuous-time function must be sampled in order to be represented in the computer. By the same reasoning, a continuous-frequency function must also be sampled in order to be represented in the computer [6],[11].

$$X(\omega) = \int x(t) e^{-jwt}\, dt \tag{2.1}$$

$$X(f) = \int x(t) e^{-j2\Pi ft}\, dt \tag{2.2}$$

In (2.2), the complex exponential is a function of time t and frequency f. To sample this function in time, replace t with nT, where T is the sampling period and n is an integer. The sampled complex exponential is then $e^{-j2\Pi fnT}$. To sample the frequency variable f, remember that sampling a signal in the time domain restricts the possible frequencies to a range of (−Fs/2, Fs/2), where Fs is the sampling rate. The continuous range of frequencies from −Fs/2 to Fs/2 can be pictured as a line from −Fs/2 to Fs/2. This is shown in the top line of Figure 2.1.

It is often more convenient to picture this range as positive frequencies from 0 to Fs. These two frequency ranges are equivalent when sampled at Fs because frequencies

above Fs/2 will alias to negative frequencies. To sample the frequency range from (0, Fs), let N be the number of frequency samples. Then the sequence ak = kFs/N, will be N evenly spaced frequency samples between 0 and Fs. A sampled frequency range for N = 8 and Fs = 32 is shown in Figure 2.1.

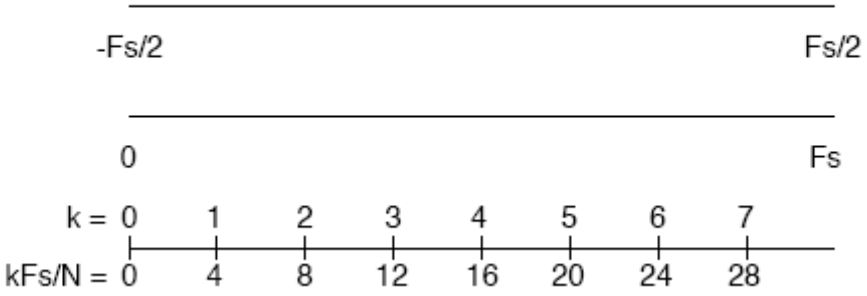

Figure 2.1: The Nyquist Interval can be pictured as a line from −Fs/2 to Fs/2. That line is the same length as a line from 0 to Fs. To get N samples from 0 to Fs, let k be an integer from 0 to N − 1 and choose the frequencies equal to kFs/N. In the lowest line, N = 8 and Fs = 32.

Mathematically, sampling the time variable t and the frequency variable f of the Fourier Transform gives the Discrete Fourier Transform shown in (2.3). The conversion of the continuous transform into the discrete transform can be represented by the steps in (2.4). The real derivation of the Discrete Fourier Transform from the Fourier Transform requires more rigor and is beyond the scope of this thesis.

$$X_d[k] = \sum_{n=0}^{N-1} x[n] e^{-j2\Pi kn/N} \tag{2.3}$$

$$X(f) = \int x(t) e^{-j2\Pi ft} dt$$

$$\rightarrow \sum_n x(nT) e^{-j2\Pi fnT}$$

$$X(kF_s / N) = \sum_n x(nT) e^{-j2\Pi kF_s nT / N}$$

$$X[k] = \sum_{n=0}^{N-1} x[n] e^{-j2\Pi kn / N} \quad (2.4)$$

The form of (2.3) is that of a scalar product. The inner product was introduced as the integral of the product of two functions. Essentially, the scalar, or dot, product is the discrete version of the inner product. It is calculated by summing the product of two discrete functions. In these terms, the Discrete Fourier Transform can be seen as the dot product of the sampled signal x[n] and the sampled basis functions $e^{-j2\Pi kn/N}$. In $e^{-j2\Pi kn/N}$, the $-2\Pi k/N$ is the frequency and n is the sample index.

In MATLAB, it is easy to calculate the Discrete Fourier Transform of a sampled signal. If the length of the signal is a power of 2, MATLAB uses the Fast Fourier Transform (FFT), an efficient algorithm for calculating the DFT.

2.2 Core Algorithm Implementation

Much like the simulation in MATLAB core algorithm is implemented first. Since it is the primary component of the proposed DPOAE estimation method, before it can be implemented in the DSP, verification of the successful implementation of the core algorithm is required [16],[19].

The core algorithm program is developed directly from the off-line MATLAB simulation. For one, the discrete equations, presented as (2.1) - (2.4), governing the algorithm are employed in the same manner. Small arrays are used to hold the current and future values of the estimated amplitude and phase. The proposed DPOAE estimation is developed around the core algorithm DSP implementation. Added to this are the necessary pre-, mid-, and post-processing stages. The same filter coefficients and difference equations are used in the same manner as in the MATLAB simulation. Normalization of the input signal is done before input to the first core algorithm units in the artifact (primary) removal stage for reasons discussed previously. Normalization and denormalization is

also employed in the mid-processing and post-processing units respectively, as in the off-line MATLAB simulation.

CHAPTER 3

DPOAE ESTIMATION METHOD AND IMPLEMENTATION

3.1 Introduction

The method of DPOAE estimation that is centered around a non- linear adaptive signal processing algorithm. Also discussed in this chapter are some details about the formulation and mathematical properties of the algorithm. Since it is essentially the "core" of the DPOAE estimation technique, the nonlinear adaptive algorithm will henceforth be referred to as the core algorithm [17].

Three core algorithm units are employed to construct this high performance method of DPOAE estimation. Each core unit is capable of extracting a pre-specified sinusoidal component of its input signal, which may consist of other components and noise. In the case of the proposed DPOAE estimation technique, the two stimuli are first extracted by two core algorithm units and subtracted from the input signal. The modified signal now has a higher relative portion of the DPOAE. This signal is then input to another core unit to estimate the level of the DPOAE signal. Extraction of these components also entails following variations in the amplitude and phase. The structure of the proposed method also includes some pre-processing, intermediate or mid-processing, and post-processing as well as some smoothing filter stages to enhance the performance.

The structure of the proposed DPOAE estimation method is simple[19]. It offers a high degree of robustness with respect to both internal and external conditions. Computer simulations used to demonstrate the superior performance of the proposed method in terms of noise immunity and fast measurement time. A comparison is made between the proposed method and a recently introduced DPOAE estimation technique presented in order to quantitatively study the high noise immunity.

The next section briefly reviews the structure of a DPOAE measurement device that can be made. The heart of such an apparatus will be the signal processing module, which contains the functional units to estimate the DPOAE signal. The performance of the structure using computer simulations and recorded data is demonstrated in section 3.3.

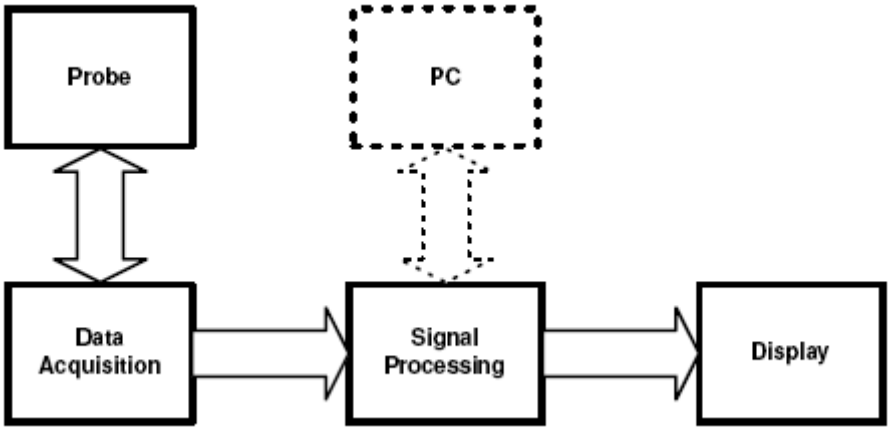

Figure 3.1: Block diagram of a DPOAE measurement device.

3.2 Structure of a DPOAE Measurement Device

Figure 3.1 shows the generic block diagram of a DPOAE measurement device. It will contain of three main modules: the data acquisition (DAQ)/transducer module, the signal processing module, and the display [13].

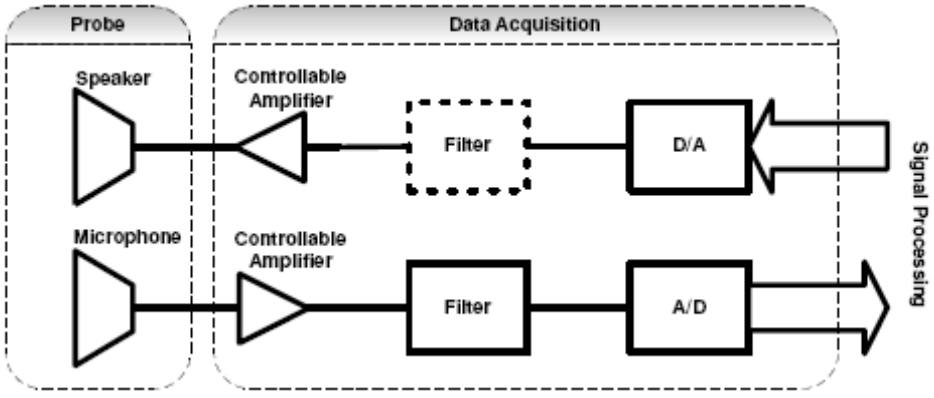

Figure 3.2: Details of a data acquisition system and probe units.

The DAQ module is the medium between the signal processing module and the probe which transmits and receives acoustic signals in the audio range. Figure 3.2 illustrates the components of the compound DAQ/transducer, or DAQ/probe module in more detail. This is where digital signals produced by the signal processing module are converted to analog signals, which are then conditioned and converted to audio signals. Conditioning usually consists of some amplification and possibly some filtering. Conversely, the returning audio signals from the microphone probe are conditioned and converted to digital signals to be processed by the signal processing module.

As mentioned previously, the signal processing module is the heart of any DPOAE estimation device [22]. It produces the digital form of the stimuli and extracts and measures the DPOAE signal. The signal processing module can take on many forms. Some of these include a DSP or a microprocessor, which would make it a hardware platform controlled by embedded software. Alternatively, if the complexity of the signal processing algorithm remains low, the signal processing module may be implemented solely in hardware using programmable logic array (PLA) or field programmable gate array (FPGA) technology.

Ideally, the personal computer (PC) module seen in Figure 3.1 would not be necessary. This is usually only possible with a signal processing algorithm that is not excessively complex. However, a PC interface is usually required for data management, making it if not a functional component of the DPOAE estimation process, then normally an essential part of the system.

The display module is the interface between the device and the operator. It could be anything from a simple light emitting diode (LED) or liquid crystal display (LCD) to a computer monitor or printer.

3.3 Proposed Technique

The proposed signal processing method employs three units of the core algorithm in order to construct a high performance DPOAE estimation algorithm. Each core unit is responsible for focusing on and extracting a predetermined sinusoidal component of its

input signal, which may contain other components and noise. More importantly, it can effectively track the amplitude and phase of the extracted sinusoidal component. In addition, the structure of the core algorithm is extremely simple, making it easy to implement in a variety of platforms. This is in contrast to its complex underlying mathematics, which ensures stability and performance [6]. The core algorithm is found to be very robust with respect to variations in the internal settings of the controlling parameters, as well as external conditions such as the presence of noise. It also exhibits superior performance over existing linear adaptive and DFT-based algorithms in terms of convergence speed versus accuracy trade-off.

The input signal to the DPOAE estimation device consists of the two primaries or stimuli (pure sinusoids) discussed earlier, the returned DPOAE (provided a normally functioning cochlea), as well as noise [17]. The high level primaries are located at f_1 and f_2 and are around 60-65 dB SPL. The low level DPOAE is located at $f_d = 2f_1 - f_2$ and is expected to be at approximately -5 to 15 dB SPL. The noise floor, which consists of background noise and all other undesirable signals, is considered to be about 0 to 20 dB SPL. An increase in estimation error occurs with an increase in the amount of stimuli and noise still present at the time the core algorithm responsible for the DPOAE estimation acts on the incoming signal. This is the primary reason for employing two more core algorithms to extract the stimuli from the incoming signal, which produces a signal with a higher relative portion of DPOAE. Readjustment of the parameters of the core algorithm is also done to improve the accuracy of the estimation process, at the expense of convergence speed.

Figure 3.3 shows the three core algorithms employed with the addition of a pre-processing, mid-processing, and post-processing stage. Their purpose is to enhance the performance of the DPOAE estimation technique by providing some simple first and second order filtering as well as normalization. The pre-processing stage consists of a second order band-pass filter and possibly some normalization. The filter is centered around f_d to attenuate everything else as much as possible, enhancing the quality of the

input signal, and in turn enabling the core algorithm units to act more accurately and efficiently.

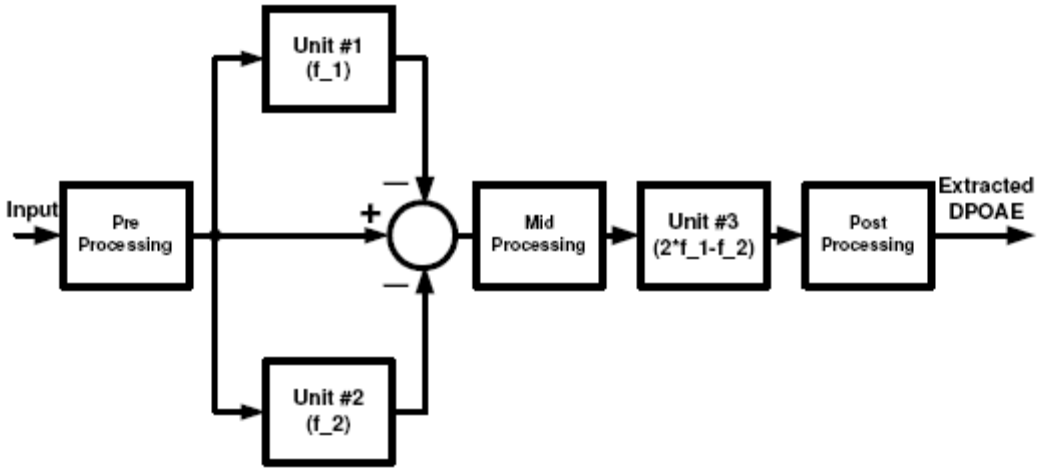

Figure 3.3: Block diagram of the original DPOAE estimation method [4].

The purpose of normalization is to amplify or attenuate the signal to bring it to a certain level, on the basis of which the parameter settings of the core algorithm units may be adjusted. The output of the pre- processing stage is input to each core algorithm set to extract the primaries located at f_1 and f_2. They accomplish this with very small errors and a very fast convergence time. The output of each of these is then subtracted from the output of the pre-processing module. Instead of letting this intermediate signal from which the two primaries are removed be the input to the third core algorithm unit, it is first sent to the mid-processing stage [24]. This is because the units removing the primaries need a certain convergence time. Therefore, at the very early initial moments, a large portion of the two primaries exists, which will set the initial operational point of the third core algorithm a significant distance from the actual DPOAE signal. This will make it extremely difficult for convergence to be achieved. In order to allow the first two core algorithm modules to converge before being sent to the third, the mid-processing stage in Figure 3.3 employs a time-gating process. The output of this unit begins at zero and remains there for a short period of time until a more or less steady state condition of the first two core algorithm units is achieved. The mid-processing unit also subjects the incoming signal to another second order band-pass filter centered at f_d ,as well as further normalization. The post-processing module consists of two first order low-pass filters and

some denormalization. Its inputs are the DPOAE signal and the level of the DPOAE signal, extracted from the third core algorithm unit. The low-pass filters are used to smooth the signals, and the normalization returns the signal and level to their proper values.

3.3.1 Core Algorithm Implementation

This section presents an overview of the core algorithm employed in the DPOAE estimation technique. The main functionality of the algorithm is to extract a non-stationary sinusoid from a signal that may contain other components and noise. This is accomplished by effectively tracking the amplitude, frequency, and phase of the extracted sinusoidal component. Let $u(t)$ denote the input signal, which is comprised of a sinusoidal component polluted by a number of undesired components and noise. Minimization of the least squares error between the sinusoidal component $Asin(\omega t + \delta)$ and the input signal $u(t)$ is used to effectively extract the embedded sinusoid. The following set of equations governs this process. These equations are what represent the nonlinear adaptive process which extracts the sinusoidal component represented as $y(t)$ from $u(t)$.

$$\dot{A}(t) = 2\,\mu_1\, e(t)\,\sin\phi(t); \tag{3.1}$$

$$\dot{\omega}(t) = 2\,\mu_2\, e(t)\,\cos\phi(t); \tag{3.2}$$

$$\dot{\phi}(t) = 2\,\mu_3\, e(t)\,\cos\phi(t) + \omega(t); \tag{3.3}$$

$$y(t) = A(t)\,\sin\phi(t); \tag{3.4}$$

$$e(t) = u(t) - y(t); \tag{3.5}$$

The dot on top ($\dot{}$) represents the differentiation with respect to time. Instantaneous estimates for the amplitude, frequency, and phase are provided by the state variables $A(t)$, $\phi(t)$, and $\omega(t)$ respectively. The error signal $e(t)$ is the result of removing the estimated sinusoid from the input, which is the combination of the noise and other undesired

components of u(t). Parameters μ_1, μ_2 and μ_3 are positive numbers that determine the behavior of the core algorithm in terms of convergence speed versus accuracy.

In the case of DPOAE estimation, three core algorithm units are employed with the purpose of either tracking one of the two primaries[19], or the DPOAE. The frequencies of the DPOAE and the two primaries are constant. Thus, these frequencies are known a priori and do not need to be tracked by the core algorithm, eliminating the need for (3.2). Further simplifying the above equations, the sinusoidal component embedded in u(t) can now be written as $Asin(\omega_0 + \delta)$, where ω_0 is the fixed frequency in radians per second.

$$\dot{A}(t) = 2\,\mu_1\, e(t)\sin\phi(t); \tag{3.6}$$

$$\dot{\phi}(t) = 2\,\mu_2\, e(t)\cos\phi(t) + \omega_0(t); \tag{3.7}$$

$$y(t) = A(t)\sin\phi(t); \tag{3.8}$$

$$e(t) = u(t) - y(t); \tag{3.9}$$

The parameters μ_1 and μ_2 are now what control the convergence speed vs. accuracy of the amplitude and phase, more of less respectively. The functionality of a system governed by (3.6) to (3.9) is essentially a notch filter in the sense that it lets pass through one specific sinusoidal component while rejecting the rest of the signal. It is adaptive due to its ability to accommodate variations in the characteristics of the desired output, including slight variations in frequency, over time. Implementation of the differential equations governing the employed core algorithm is straightforward. Figure 3.4 shows the schematic of the core algorithm. For simulations used in this chapter, MATLAB simulink is used as the main computational tool. One can see that the algorithm essentially consists of a few arithmetic and trigonometric operations, which may be easily implemented in any programming language.

An important aspect of the performance of the algorithm is its settling time, or the time it takes to settle within a certain percentage of its steady state response. A physical system approaches steady state within a few multiples of its time constant $\tau = 1/\mu$, where μ

denotes the eigenvalue of the system. The eigenvalues of the core algorithm are $-\mu_1/2$ and $-\mu_2/2A$ (A being the amplitude of the extracted sinusoid), which determine the settling time. If $\mu_1 = \mu_2 = 20000$, the system should reach steady state in about $5\tau = 1$ ms for an input signal of unit amplitude. In the case of an input signal consisting of a single pure sinusoid, the values of μ_1 and μ_2 can be chosen large so as to increase the speed of convergence without any trade-off of accuracy.

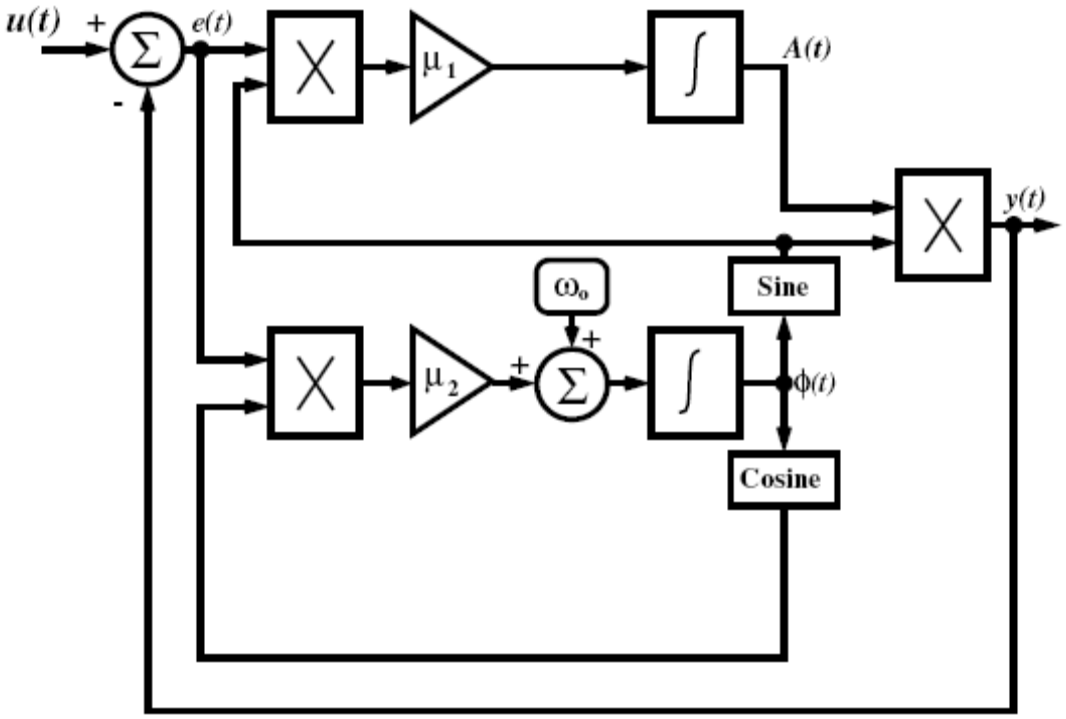

Figure 3.4: Block diagram representation of the employed core algorithm [41].

However, as the pollution increases in the input signal, or in other words, the signal to noise ratio (SNR) decreases, the trade-off between speed and accuracy will also increase. For example, if the same parameters were used on an input polluted with a zero-mean white Gaussian noise of 100% relative magnitude (i.e. $\sigma = 1/\sqrt{2}$), the output will have a 5% error in terms of its amplitude. However, if the specifications of the application could accept a reduction in convergence time, the μ parameters can be reduced to compensate for this error. The reduction of the parameters by a factor of 100 led to a convergence time of about 100 times longer and a decrease in error by a factor of 10. Therefore,

adjustment of the controlling parameters μ_1 and μ_2 provides a means of balancing the speed vs. accuracy trade-off when pollution exists in the input signal. One must keep in mind that the higher degree of pollution in the input signal causes a less desirable trade-off between the speed and accuracy and vice versa. Choosing what μ-parameters are right for different applications depends on the quality of the input signal, and particular applications specifications in terms of the desired convergence time and/or the tolerable steady state error.

The core algorithm is very insensitive with respect to variations in the μ-parameters, or alternately with respect to variations in the characteristics of the input signal. This presents a high degree of robustness in terms of internal conditions. Likewise, and because of the adaptive nature of the algorithm, variations in the characteristics of the input signal are effectively tracked over time. This presents a high degree of robustness with respect to external conditions. These characteristics are inherent in the proposed DPOAE estimation technique since it is built upon the core algorithm.

3.3.2 Variation of Parameters

Optimal performance of the DPOAE estimation method requires the adjustment of the parameters of the core algorithm. As stated earlier, one has to define the nature of the input signal and the desired convergence speed (and/or tolerable error) to properly perform the adjustment. The input consists of the primaries, which are at a known level 60 to 65 dB, the DPOAE, and noise. For initial adjustments, the DPOAE is expected to be around 15 dB and the noise floor at about 10 dB. A convergence time of less than one second for each DPOAE level measurement and an estimation error of less than 15% seem practical and are sufficient to enable the proposed method to be superior to other DPOAE estimation techniques. These definitions are rough guidelines for the design. However, thanks to the robust and adaptive nature of the core algorithm, and hence the DPOAE estimation method, variations of orders of magnitude in these values are easily tolerated by the system. The pre-processing stage, as mentioned before, consists of a simple second order band-pass filter.

Using the above mentioned input level and application specifications, the core algorithm unit parameters are adjusted. In the case of the two core units assigned to extract the primaries, μ_1 = 200 and μ_2 = 20000. The values of the μ-parameters assigned to extract the DPOAE signal are μ_1 = 200 and μ_2 = 20.

The mid-processing stage consists of time-gating, normalization, and band-pass filtering. The time-gate is set to allow the mid-processing input to continue to the rest of the system at t = 100 ms. Normalization is a simple gain of 1000. Its purpose is to bring the level of the intermediary signal to the order of 10^0. This helps the adjustment of the values of the μ-parameters. Without the gain, different values would have to be determined.

The estimate of the DPOAE signal and its amplitude by the third core algorithm unit is transferred to the post-processing module. Denormalization by attenuating by a factor of 1000 places the DPOAE signal and the amplitude of the DPOAE on a level in accordance with the original system input. The outputs of the smoothing low-pass filters are the estimated DPOAE signal and level.

3.4 Simulation

DPOAE level estimation is usually based on a number of measurements at different frequencies. A graph presenting the level of the DPOAE as a function of frequency provides a rough sketch of the transfer function of the ear. Normally, the frequency range of the two primaries, and in turn the DPOAE is in the auditory range. For the simulations presented in this section, the frequency of the first primary ($f1$) ranges from 500 to 4000 Hz and is randomly generated for each numerical experiment. The frequency of the second primary is set to $f_2 = 1.2 f_1$, and the frequency of the DPOAE to $f_d = 2 f_1 - f_2$. The initial phase of the simulated stimuli (primaries) and the DPOAE are randomly chosen within 0 to $2\prod$. The simulated noise added to the input signal is a zero-mean white Gaussian noise (for most cases).

The frequencies of the two primaries are f_1 = 2000 Hz and $f_2 = 1.2 f_1$ = 2400 Hz. The frequency of the expected DPOAE is $f_d = 2 f_1 - f_2$ = 1600 Hz. The μ parameters for the core algorithm units responsible for extracting the primaries are set to μ_1 = 200 and μ_2 = 10000, while the μ - parameters for the core algorithm responsible for extracting the DPOAE are μ_1 = 200 and μ_2 = 20. The sampling frequency is set to f_s = 24000 Hz, which will be the actual sampling frequency used by the audio daughter card.

The equations presented in this chapter that govern the dynamics of the core algorithm can not be used in their original form in a discrete environment such as MATLAB. Therefore, discrete versions of (3.6) - (3.9) that describe the dynamics of the algorithm are required.

These equations are as follows:

$$y[n] = A[n] \sin \phi[n]; \tag{3.10}$$

$$e[n] = u[n] - y[n]; \tag{3.11}$$

$$A[n+1] = A[n] + 2 T_s \mu_1 e[n] \sin \phi[n]; \tag{3.12}$$

$$\phi[n+1] = \phi[n] + T_s \omega_0 + 2 T_s \mu_2 [n] \cos \phi[n]: \tag{3.13}$$

For the above equations, *u* is the input signal, *y* is the output signal, *e* is the error signal, *A* is the estimated amplitude, ϕ is the estimated phase, ω_0 is the frequency of the desired sinusoid to be tracked in rad/s, and *Ts* is the sampling period; μ_1 and μ_2 are the controlling parameters of the algorithm that adjust the convergence speed versus accuracy trade-off discussed in this chapter. In terms of the amplitude and phase, the derivatives present in (3.6) and (3.7) are replaced by their first order approximations:

$$\dot{A}(t) \approx \frac{A[n+1]-A[n]}{T_s}$$

$$\dot{\phi}(t) \approx \frac{\phi[n+1]-\phi[n]}{T_s}$$

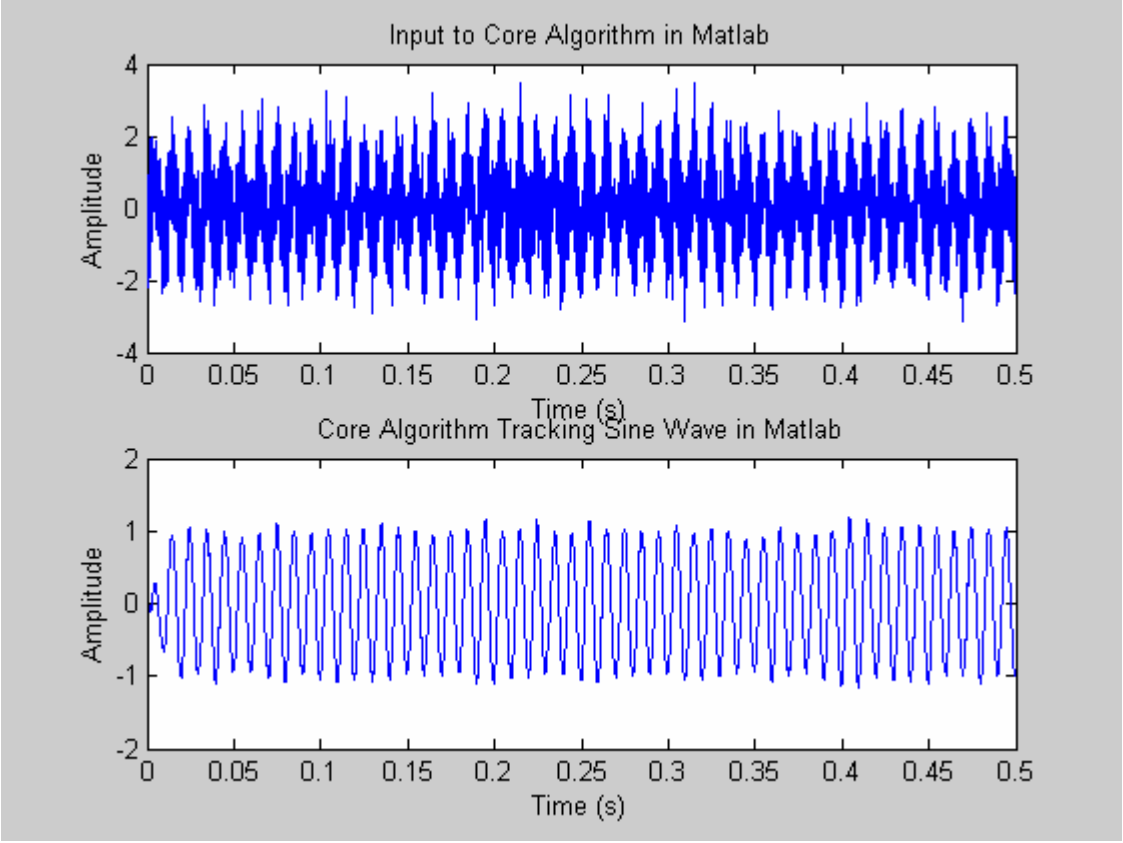

Figure 3.5: Illustration of the performance of the discrete core algorithm in Matlab with $\mu_1 = \mu_2 = 200$

The algorithm is structured to take one input value, process it, and output it before processing the next input value. The input signal to the algorithm consists of a sinusoid with a random constant phase and the optional addition of a white Gaussian noise. A simple call to the MATLAB "sin" function in the form of u = sin(2*$\prod$*f_0 *$dt+\delta$) + $e[n]$, where f_0 is the frequency of the desired sinusoid to be tracked in Hz, dt is the

particular moment in time, δ is the random constant phase, and $e[n]$ is the value of the noise for that particular sampling period, generates the input signal. The noise vector is generated by the MATLAB “randn" function, which generates a set of zero-mean normally distributed random numbers. Each time a sample is processed, *dt* must be increased by *Ts* to simulate the next value at the next sampling period of the input sine wave. Figures 3.5 and 3.6 demonstrate the performance of the discrete core algorithm with added noise of 100% relative magnitude and unit amplitude for the input sinusoids.

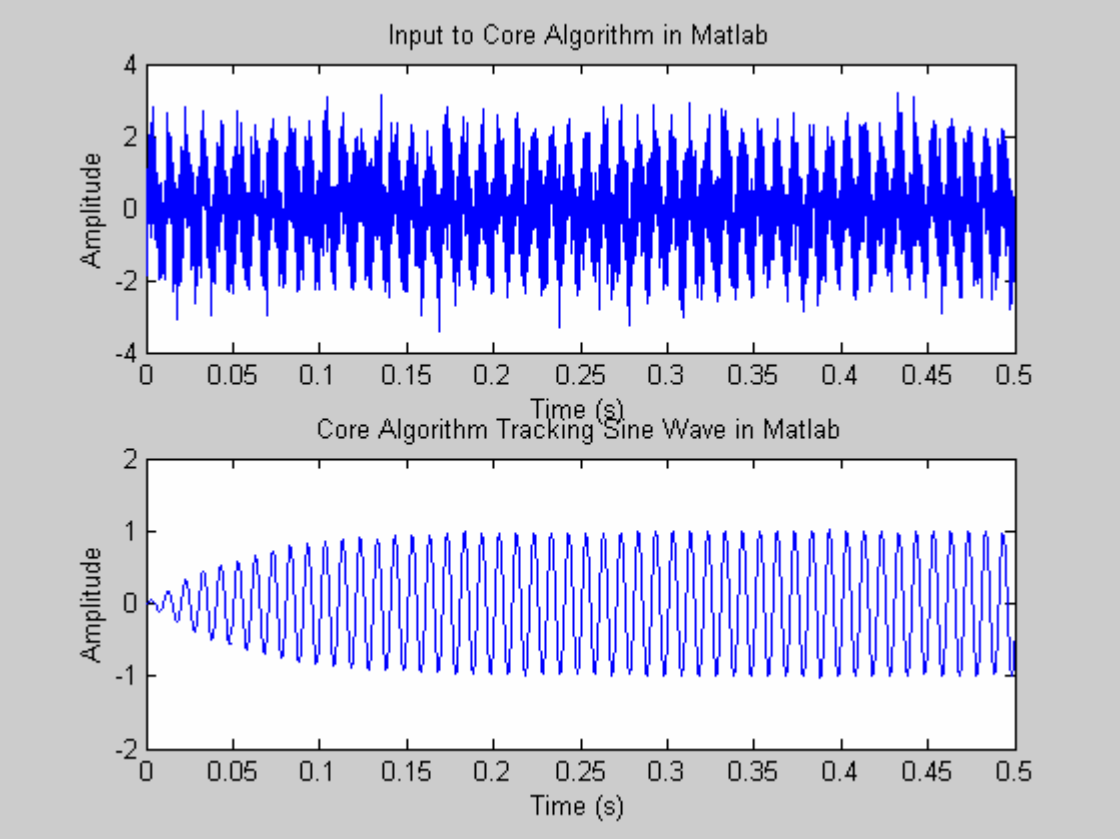

Figure 3.6: Illustration of the performance of the discrete core algorithm in Matlab with $\mu_1 = \mu_2 = 20$

Figure 3.5 shows the performance of the algorithm when $\mu_1 = \mu_2 = 200$, and Figure 3.6 illustrates the performance when $\mu_1 = \mu_2 = 20$. One can observe the algorithm successfully extracting a sine wave in both cases, with the first case having a faster convergence time, but also a slightly higher estimation error.

3.5 Filter Design

Referring to Figure 3.3, besides the three core algorithm units needed for DPOAE estimation, a pre-, mid-, and post-processing stage is also required. Each stage, in addition to some other functionality, involves a type of filtering which is essential for the core algorithm units to be effective[19]. Even though MATLAB is capable of implementing filters in many different forms, eventually these filters must be employed in a DSP program, which requires the use of difference equations. Therefore, this section discusses the design of digital flters and the development of their subsequent difference equations for the proposed DPOAE estimation method [20].

The original filters present in the continuous block diagram are in the form of transfer functions in the analog, or *s*-domain. The equations for the transfer functions of the pre-processing, mid-processing, and post-processing DPOAE and level filters are

$$H_{pre}(s) = \frac{100s}{s^2 + |100s + 2\prod f_d} \tag{3.14}$$

$$H_{mid}(s) = \frac{10s}{s^2 + 10s + 2\prod f_d} \tag{3.15}$$

$$H_d(s) = \frac{1}{.0001s + 1} \tag{3.16}$$

$$H_l(s) = \frac{1}{.05s + 1} \tag{3.17}$$

Where f_d is the DPOAE frequency of $f_d = 2f_1 - f_2$. These transfer functions contain information that is used with the Filter Design and Analysis (FDA) Tool, present in the Matlab Signal Processing Toolbox, to develop the coefficients for the discrete transfer function in the *z*-domain. Specifically, the orders of (3.14) through (3.17), the center

frequency and the bandwidth of the filters described by (3.14) and (3.15), and the cutoff frequencies of the fiters described by (3.16) and (3.17), are used as the inputs to the FDA Tool. The orders of these equations can easily be determined by the highest exponent on an *s*-term. Thus, the band-pass filters represented by (3.14) and (3.15) are second order, and the low-pass filters represented by (3.16) and (3.17) are first order. The bandwidth of the band-pass filter is given by the coefficient present in the numerator, and the center frequency is established by the last term in the denominator, or f_d. The bandwidth B is defined as $B = \Omega_H - \Omega_L$, where Ω_H is the upper 3 dB point, or cutoff frequency, and Ω_L is the lower in radians. Therefore, in the case of the pre-processing filter, B = 100, and for the mid-processing filter, B = 10. Converting the center frequency to radians by letting $\Omega_D = 2\prod f_d$ = 10,053, the upper and lower 3 dB points can be determined by $\Omega_H = \Omega_D + \frac{B}{2}$ and $\Omega_L = \Omega_D - \frac{B}{2}$. This yields upper and lower cutoff frequencies of Ω_H = 10,103 and Ω_L = 10; 003 for the pre-processing filter, and Ω_H = 10,058 and Ω_L = 10,048 for the mid-processing filter. Since the FDA Tool takes these inputs in Hz, the equation $f = 2\prod/\Omega$ is used to determine the translated upper and lower cutoff frequencies of f_h = 1608 Hz and f_l = 1592 Hz for the pre-processing filter, and f_h = 1600.8 Hz and f_l = 1599.2 Hz for the mid-processing filter. These values, along with a second order band-pass filter type and a sampling frequency of f_s = 24,000, are the inputs to the FDA Tool. The design method is chosen as an infinite impulse response (IIR) Butterworth filter. Choosing IIR will keep the order of the digital filter relatively low, which will be very important during DSP implementation in terms of execution speed[24]. A Butterworth filter has a monotonic response in the pass and stop bands [24], eliminating the concern for any ripple effect. As for the two first order low-pass filters in the post-processing stage, the cutoff frequency f_c is needed for the FDA Tool to compute the coefficients. First, the analog transfer functions of the filters need to be transformed into the form

$$H(s) = \frac{\Omega_c}{s + \Omega_c}$$

Where $\Omega_c = 2\prod f_c$, or the cutoff frequency in radians. Performing this conversion on (3.16) and (3.17) yields

$$H_d(s) = \frac{10{,}000}{s + 10{,}000} \tag{3.18}$$

$$H_l(s) = \frac{20}{s + 20} \tag{3.19}$$

From (3.18) and (3.19), f_c is derived for the DPOAE signal low-pass filter as f_c = 1591.5 Hz, and for the level low-pass filter as f_c = 3.1831 Hz. Other inputs required for the FDA Tool are kept the same as the band-pass filters, except of course for the order which is set to 1. In the end, the discrete transfer functions for the pre-, mid-, and post-processing digital filters are

$$H_{pre}(z) = \frac{.0021 - .0021z^{-2}}{1 - 1.8237z^{-1} + .9958z^{-2}} \tag{3.20}$$

$$H_{mid}(z) = \frac{.0002 - .0002z^{-2}}{1 - 1.8267z^{-1} + .9996z^{-2}} \tag{3.21}$$

$$H_d(z) = \frac{.1745 + .1745z^{-1}}{1 - .6510z^{-1}} \tag{3.22}$$

$$H_l(z) = \frac{.0004 + .0004z^{-1}}{1 - .9991z^{-1}} \tag{3.23}$$

It is from these discrete transfer functions that difference equations are directly derived to be used in the MATLAB simulation. Using the transfer function

$$H(z) = \frac{Y(z)}{X(z)} \tag{3.24}$$

Where $Y(z)$ is the output and $X(z)$ is the input in the frequency domain, the difference equations for each filter are derived by setting (3.24) equal to (3.20) through (3.23), cross multiplying the numerators and denominators, and taking the inverse z-transform. This yields the following difference equations for the pre-processing, mid-processing, post-processing DPOAE signal, and post-processing level filters respectively:

$$Y_{pre}(n) = a_{pre}x_{pre}[n] - a_{pre}x_{pre}[n-2] + b_{1pre}y_{pre}[n-1] + b_{2pre}y_{pre}[n-2] \tag{3.25}$$

$$Y_{mid}(n) = a_{mid}x_{mid}[n] - a_{mid}x_{mid}[n-2] + b_{1mid}y_{mid}[n-1] + b_{2mid}y_{mid}[n-2] \tag{3.26}$$

$$Y_d[n] = a_d x_d[n] + a_d x_d[n-1] + b_d y_d[n-1] \tag{3.27}$$

$$Y_l[n] = a_l x_l[n] + a_l x_l[n-1] + b_l y_l[n-1] \tag{3.28}$$

Where

$a_{pre} = .0021;\ b_{1pre} = 1.8233;\ b_{2pre} = .9958;$

$a_{mid} = .0002;\ b_{1mid} = 1.8267;\ b_{2mid} = .9996;$

$a_d = .1745;\ b_d = .6510;$

$a_l = .0004;\ b_l = .9992;$

For programming purposes, 8 arrays are declared to hold the numerator and denominator coefficients for each filter, and references are made to the arrays in the difference equations.

Also, arrays are declared for each input (x) and output (y) vector. In the case of the pre-processing and mid-processing band-pass filters, these arrays are three elements to account for being second order, which requires the current (n) and two most recent (n-1 and n-2) values to be stored. For the post-processing low-pass filters, only two elements are needed, the current and previous values. It is important to note that the MATLAB simulation is operating in a simulated real-time manner. This requires a time shift before each subsequent value is input to the filter. In the case of the pre-processing and mid-processing filters, four lines of code are needed for the input and output shift, and are of the form

$$x[n - 2] = x[n - 1];$$
$$x[n - 1] = x[n];$$

$$y[n - 2] = y[n - 1];$$

$$y[n - 1] = y[n];$$

Since the post-processing filters are first order, only the $x[n - 1] = x[n]$ and $y[n - 1] = y[n]$ shifts are required for these cases.

3.6 Time-Gating

The proposed DPOAE estimation algorithm requires a time-gating process in the mid-processing stage before the normalization and band-pass filter. Its purpose is to allow the first two core algorithm units, which are responsible for the extraction of the primaries, time to converge. Without this, the third core algorithm unit will begin the extraction process too far away from the actual DPOAE level and have a much more difficult time converging. Computer simulations using schematic software tools with the block diagram representation of the DPOAE estimation method shows that a delay of 100 ms is enough time for the convergence of the first two core algorithm blocks.

3.7 Input Signal Generation

The input signal for the MATLAB simulation is generated in the same way as the core algorithm MATLAB simulation. However, instead of one sinusoidal input, there are three. The primaries are located at f_1 = 2000 and f_2= 1.2 f_1 = 2400, and the DPOAE signal is at f_d = 2 f_1 - f_2 = 1600. The two primaries are of unit amplitude, and the DPOAE sinusoid is given an amplitude of .006. Assuming that unit amplitude corresponds to 60 dB, .006 is roughly 15 dB, which would symbolize a strong DPOAE signal emitted from a healthy cochlea. Each sinusoid is also given a random constant phase. To simulate testing in a noisy environment, a zero-mean white Gaussian noise is added. The noise vector is once again created using the “randn" function. Changing the coefficient of the noise will change its relative magnitude, essentially raising or lowering the noise floor. This permits the testing of the performance of the proposed DPOAE estimation process in environments containing various levels of background noise

CHAPTER 4

SIMULATION RESULTS

4.1 Simulation Results

First DFT implementation is done using Hamming and Rectangular Windows. Figure 4.1 show plots of different 16,32,128-point DFTs produced by the MATLAB simulations using Hamming Window and figure 4.2 show plots of different 16,32,128-point DFTs produced by the MATLAB simulations using Rectangular Window.

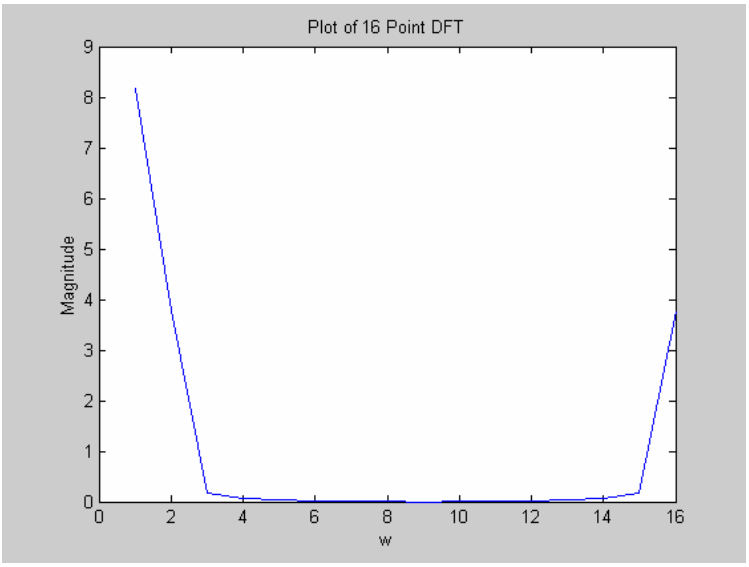

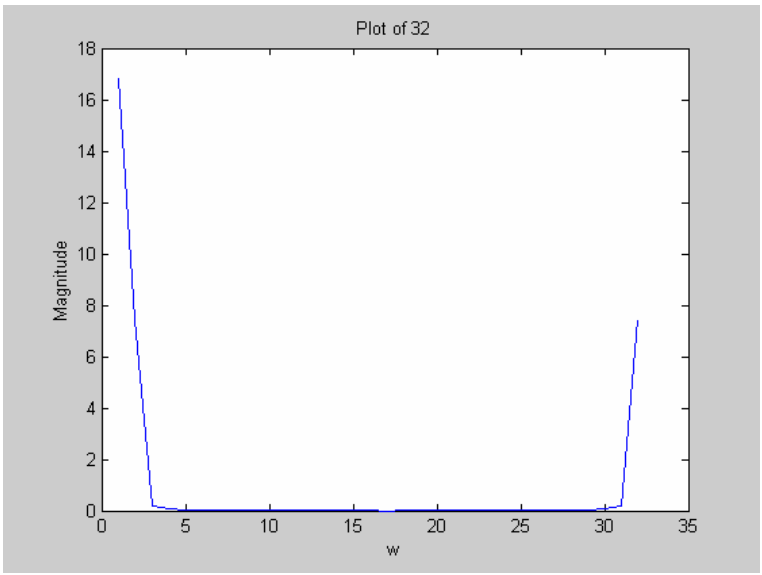

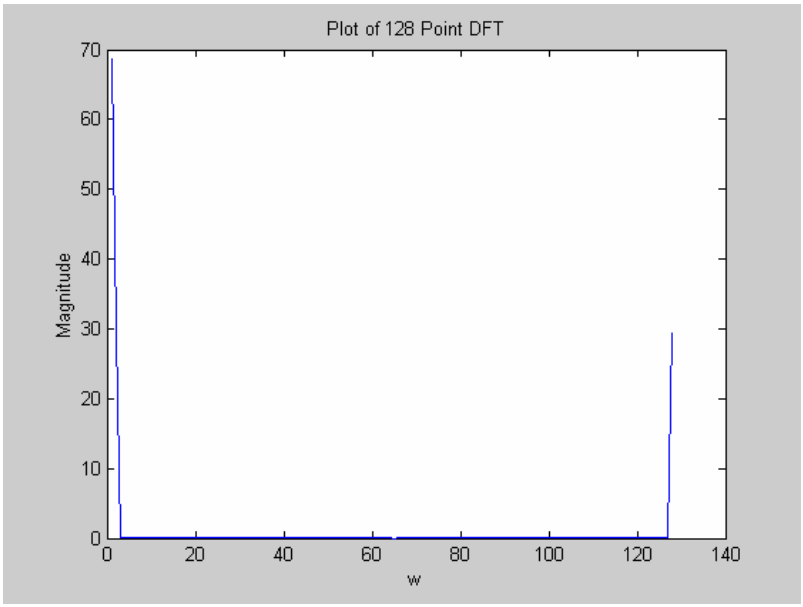

Figure 4.1: Illustration of a 16, 32 and 128 point DFT by using Hamming Window

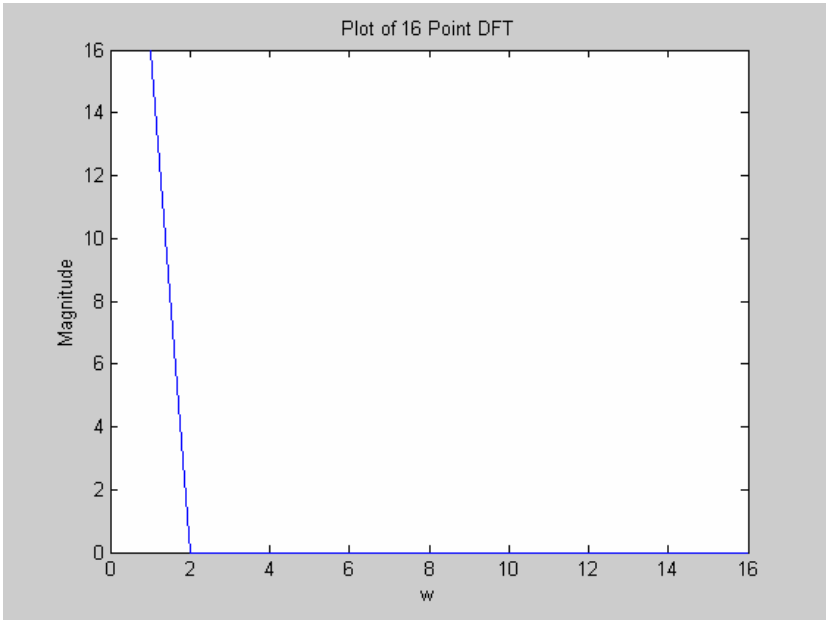

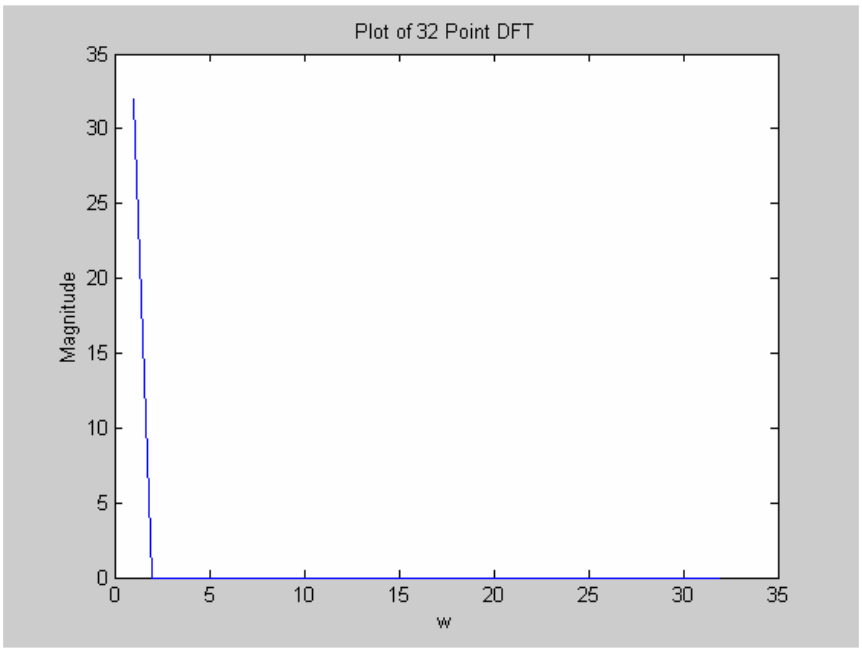

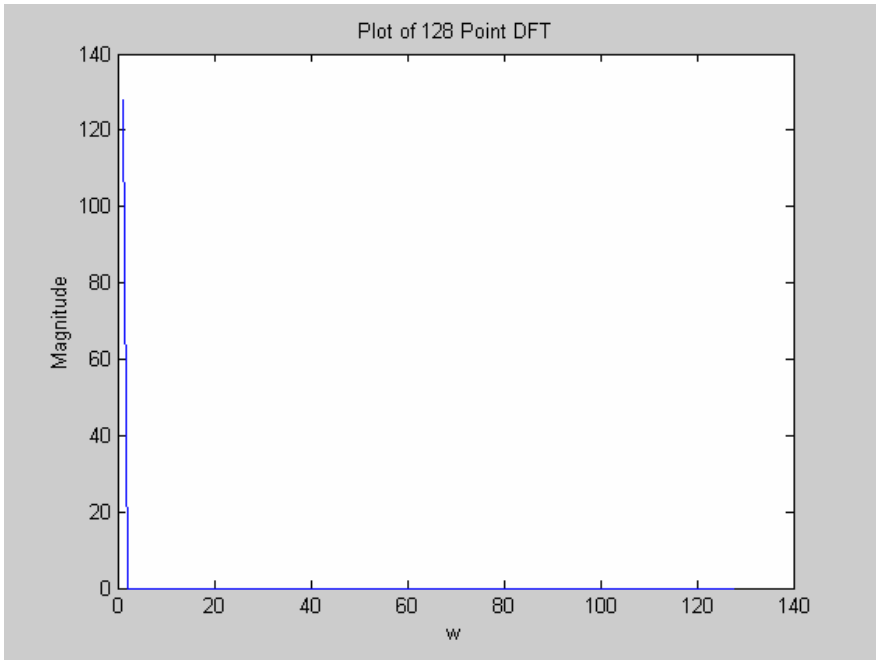

Figure 4.2: Illustration of a 16, 32 and 128 point DFT by using Rectangular Window

4.2 Results for Input Signal

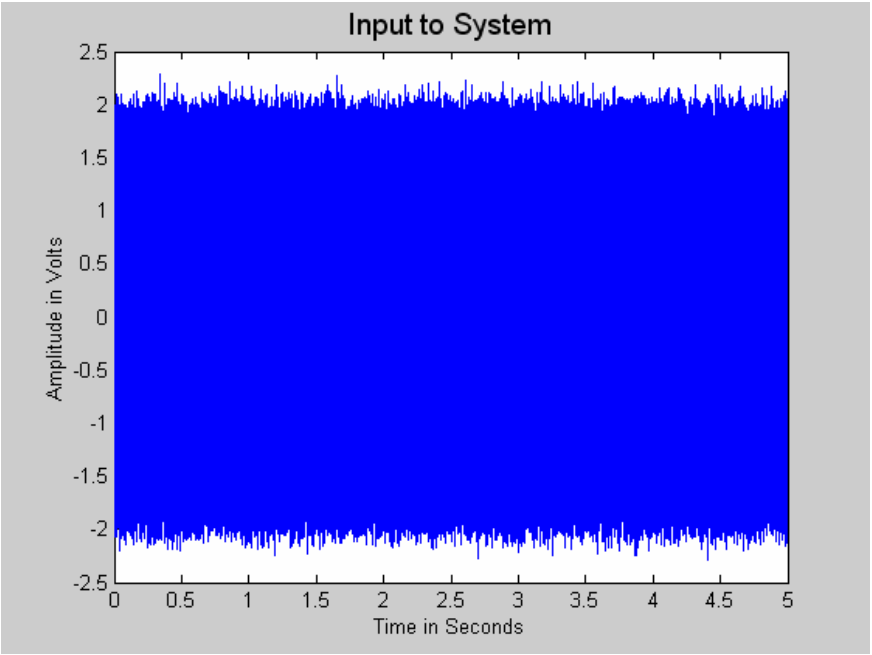

Figure 4.3: Illustration of a magnified view of the input signal with a low noise floor with f_1=1000Hz

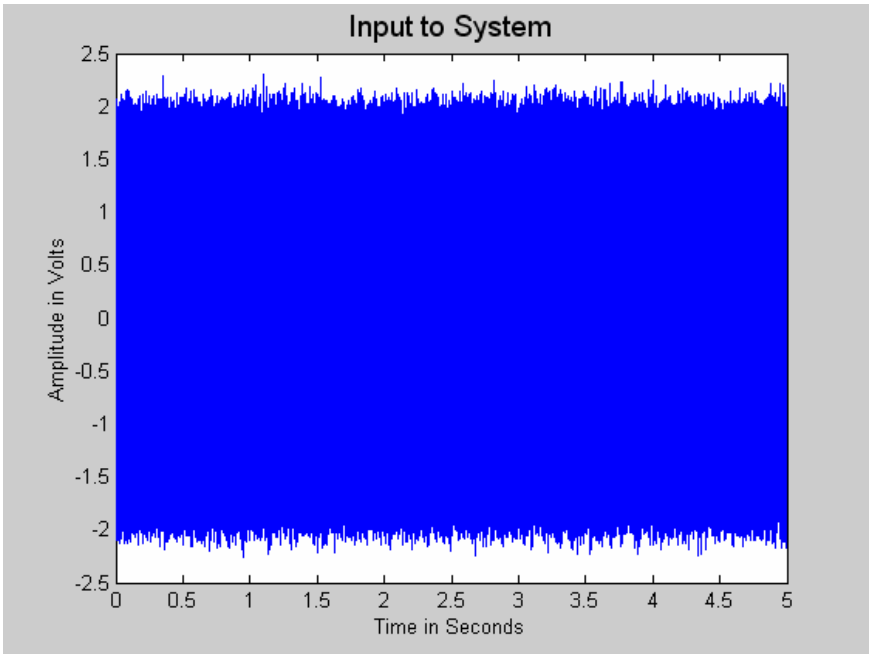

Figure 4.4: Illustration of a magnified view of the input signal with a low noise floor with f_1=2000Hz

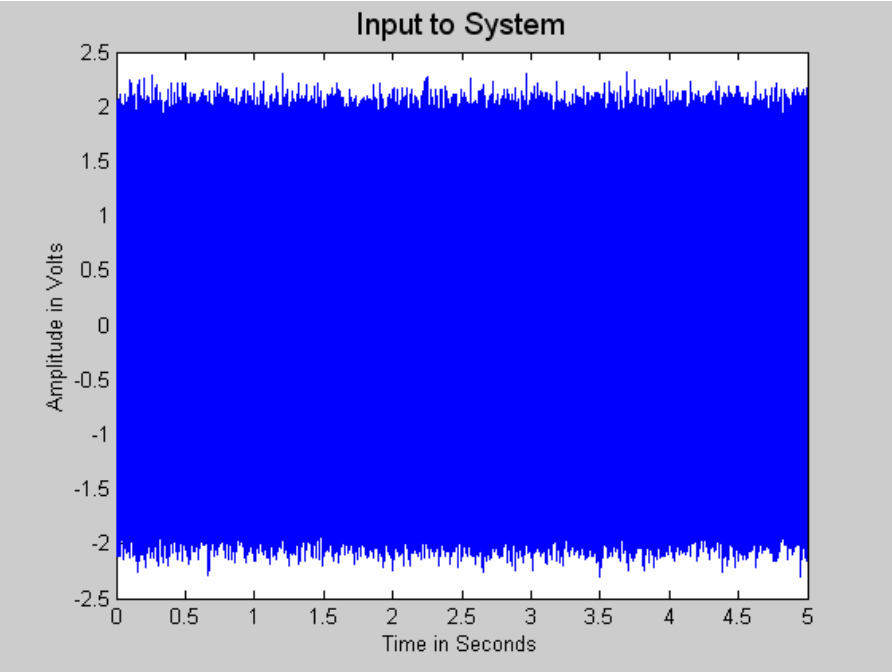

Figure 4.5: Illustration of a magnified view of the input signal with a low noise floor with f_1=3000Hz

4.3 Results for Frequency Content Of Input Signal

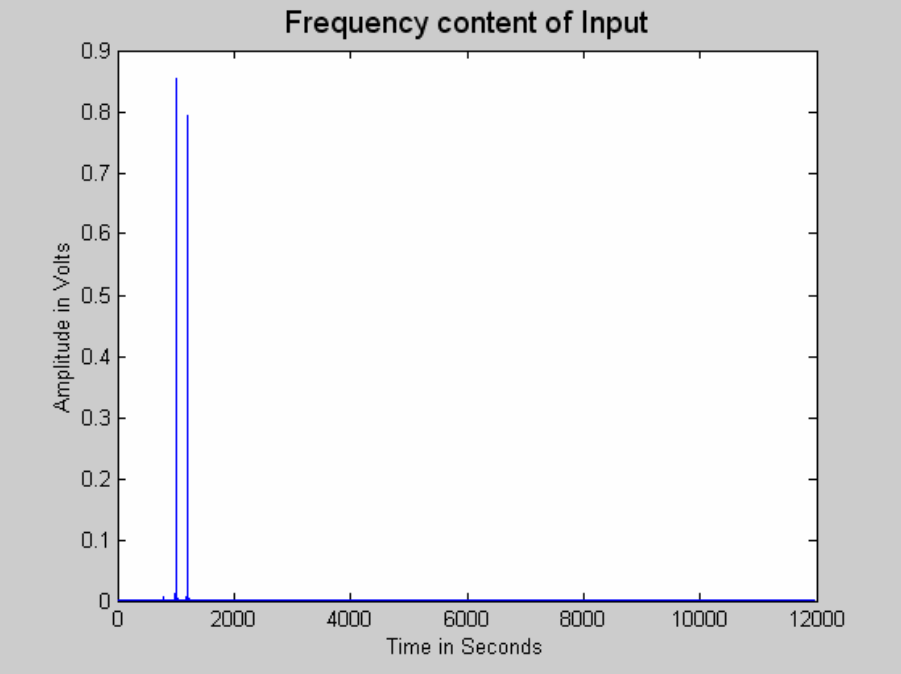

Figure 4.6: Illustration of a frequency content of the input signal with f_1=1000Hz

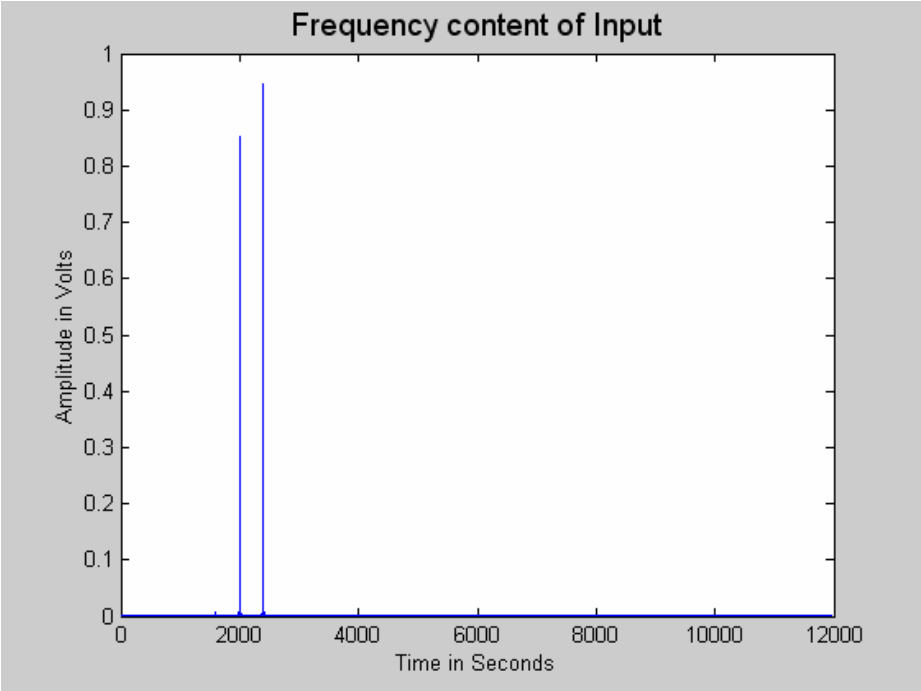

Figure 4.7: Illustration of a frequency content of the input signal with f_1=2000Hz

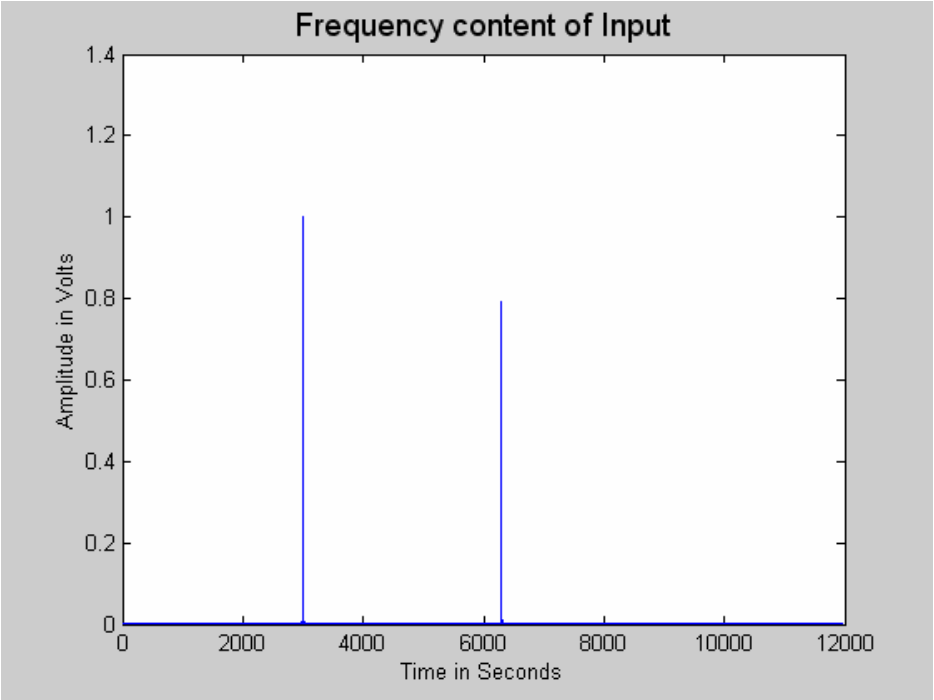

Figure 4.8: Illustration of a frequency content of the input signal with f_1=3000Hz

4.4 Results for output of pre-processing BPF

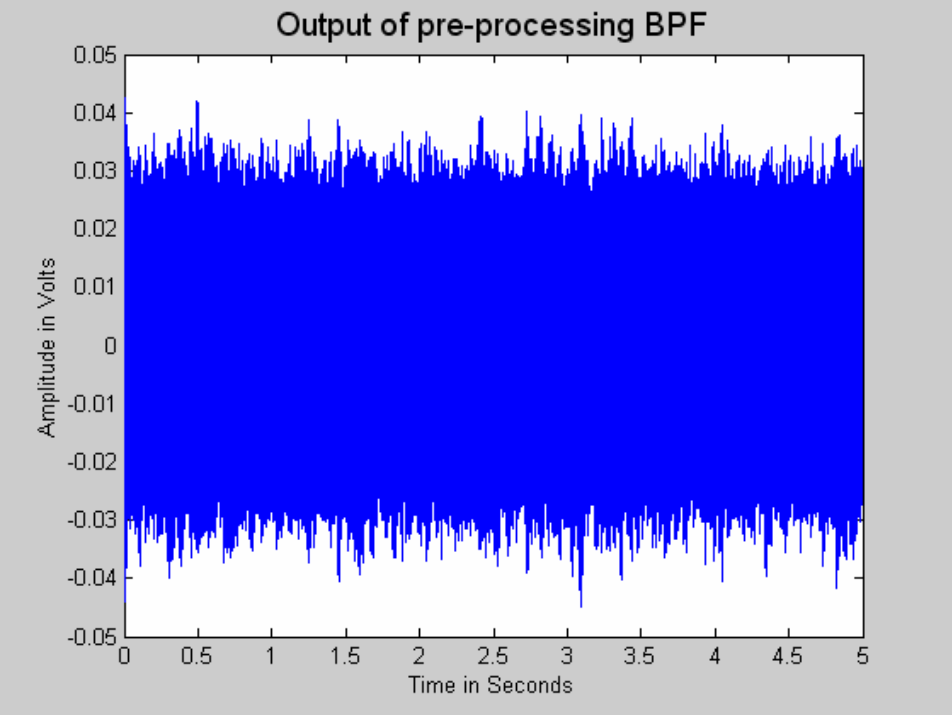

Figure 4.9: Illustration of the output of pre-processing BPF with f_1=1000Hz

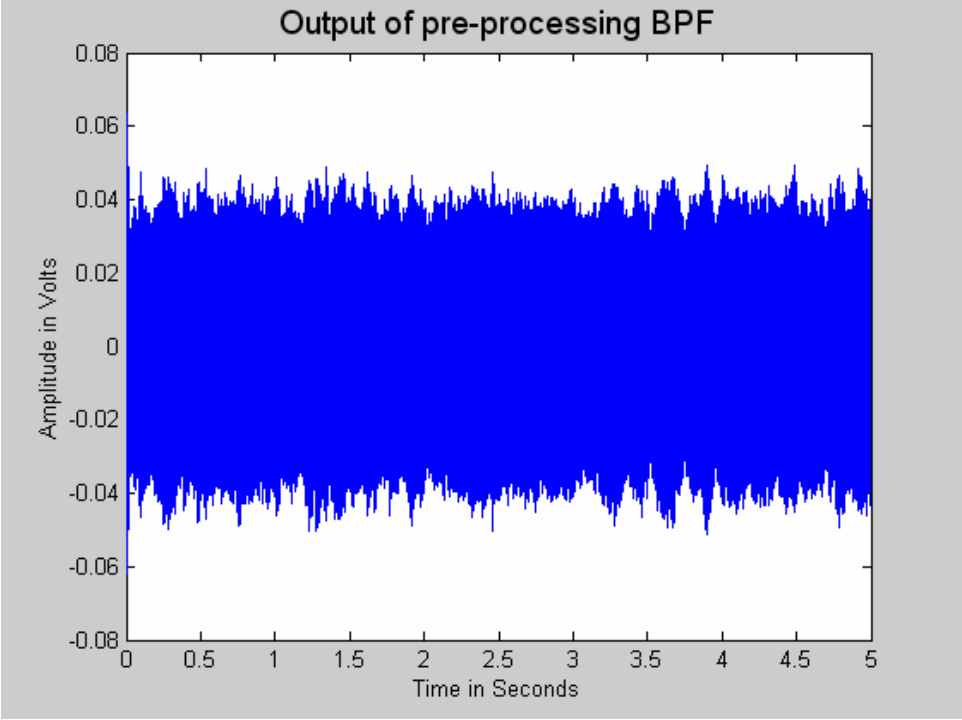

Figure 4.10: Illustration of the output of pre-processing BPF with f_1=2000Hz

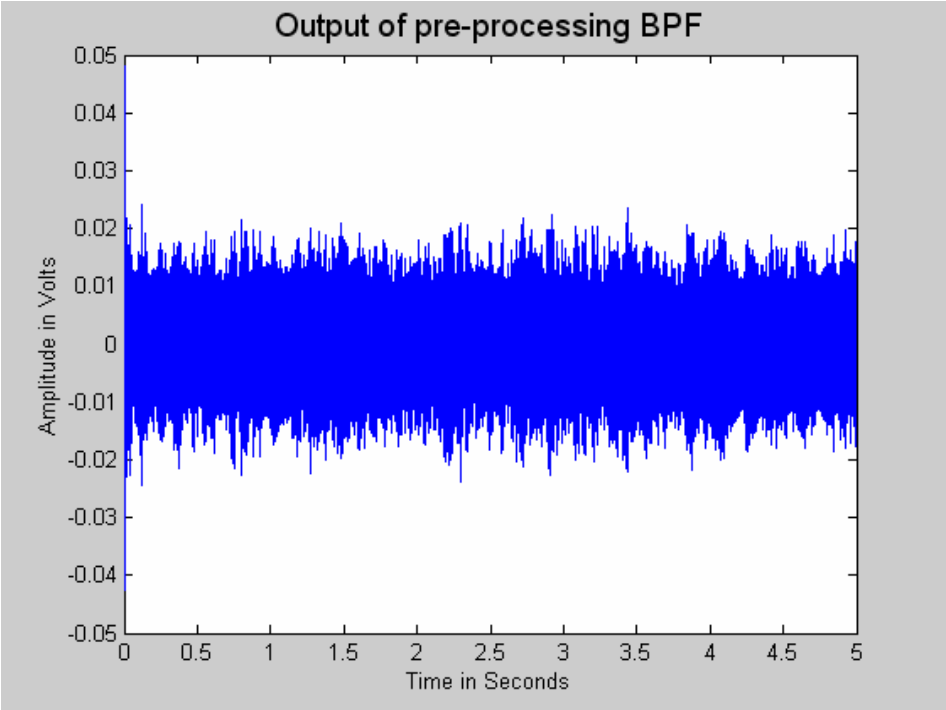

Figure 4.11: Illustration of the output of pre-processing BPF with f_1=3000Hz

4.5 Results for frequency content output of pre-processing BPF

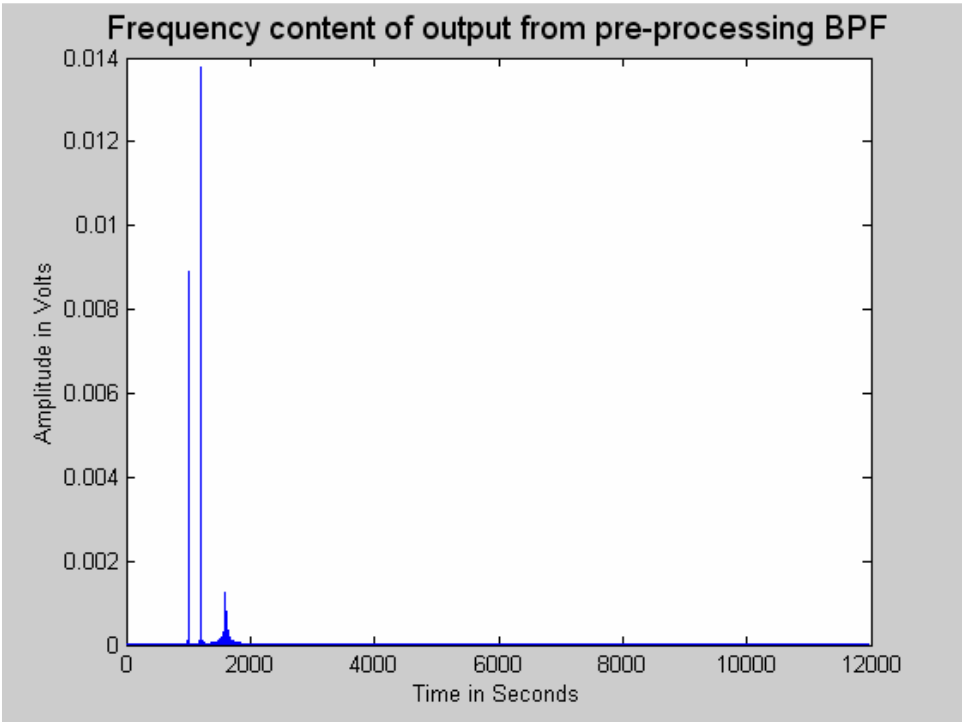

Figure 4.12: Illustration of a frequency content of the output from pre-processing BPF with f_1=1000Hz

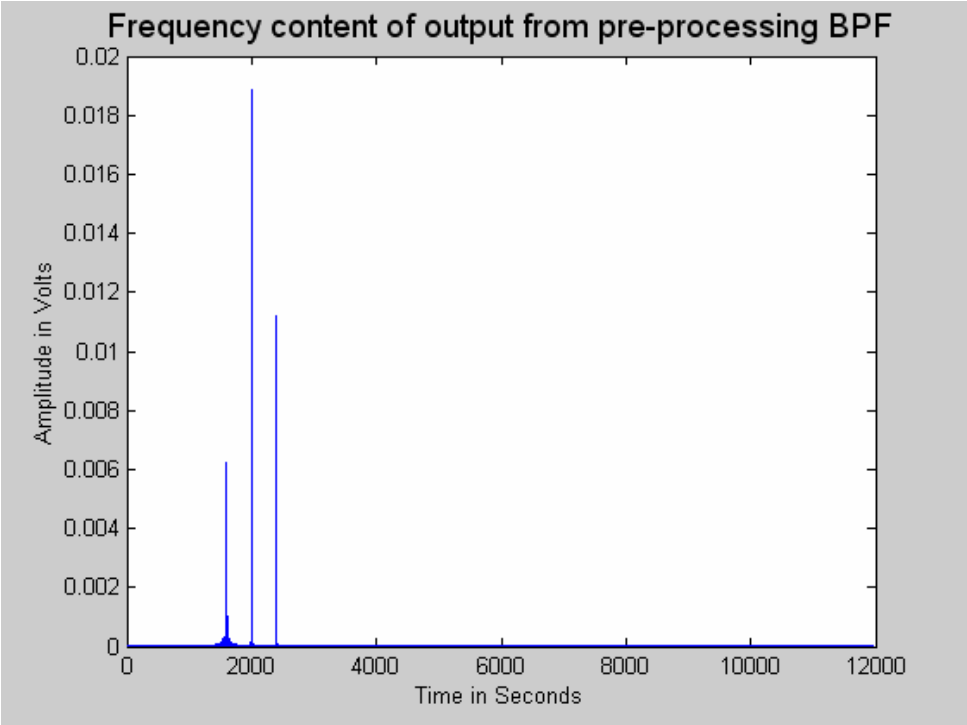

Figure 4.13: Illustration of a frequency content of the output from pre-processing BPF with f_1=2000Hz

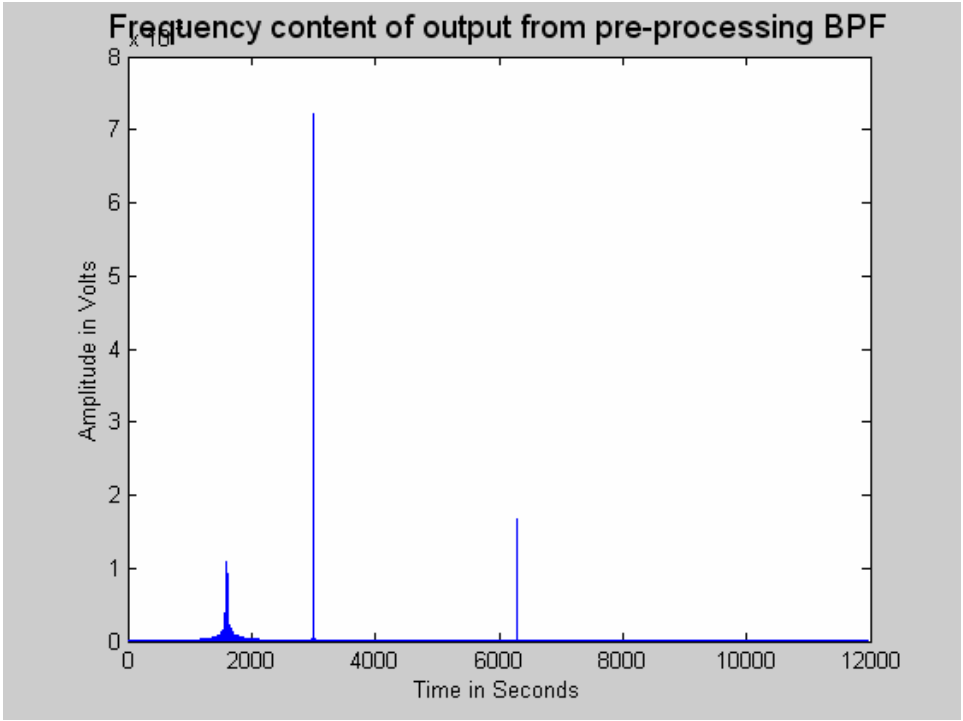

Figure 4.14: Illustration of a frequency content of the output from pre-processing BPF with f_1=3000Hz

4.6 Results for output of artifact removal

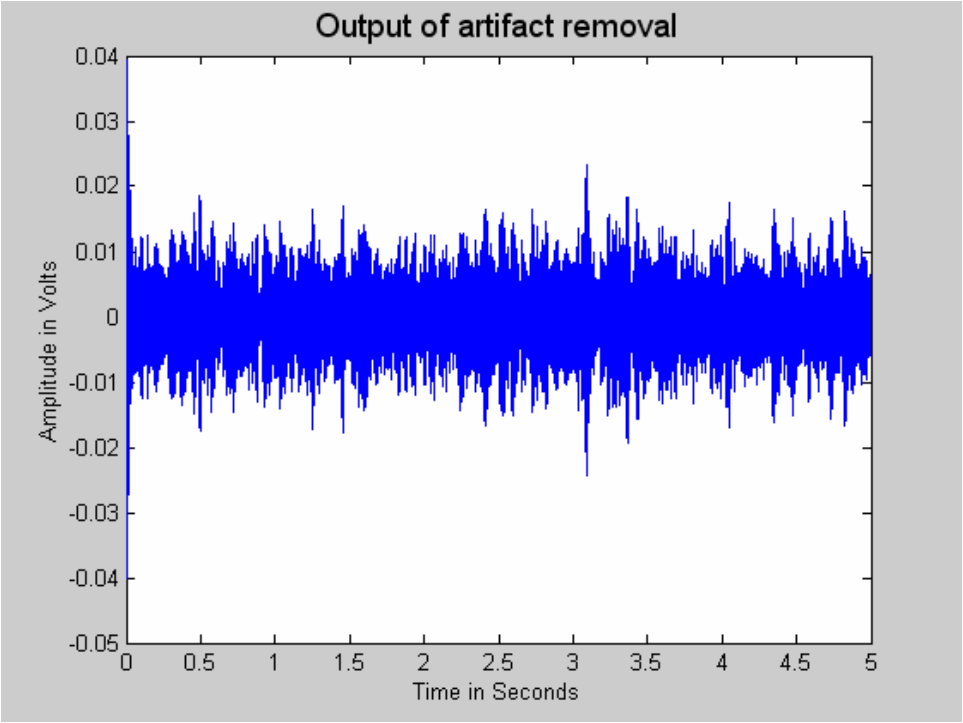

Figure 4.15: Illustration of the output of artifact removal with f_1=1000Hz

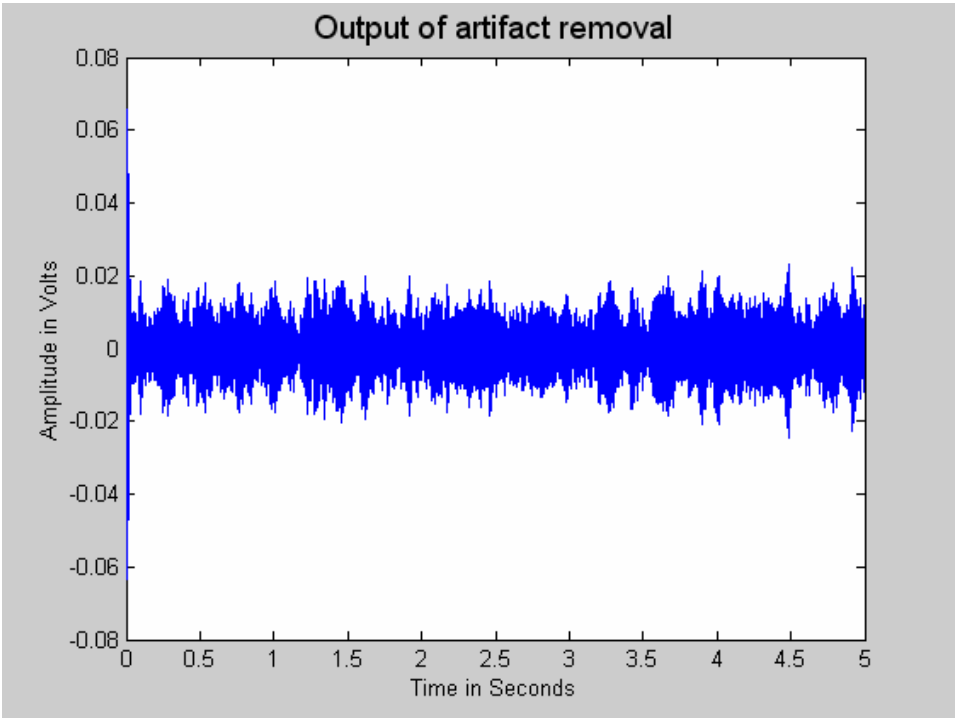

Figure 4.16: Illustration of the output of artifact removal with f_1=2000Hz

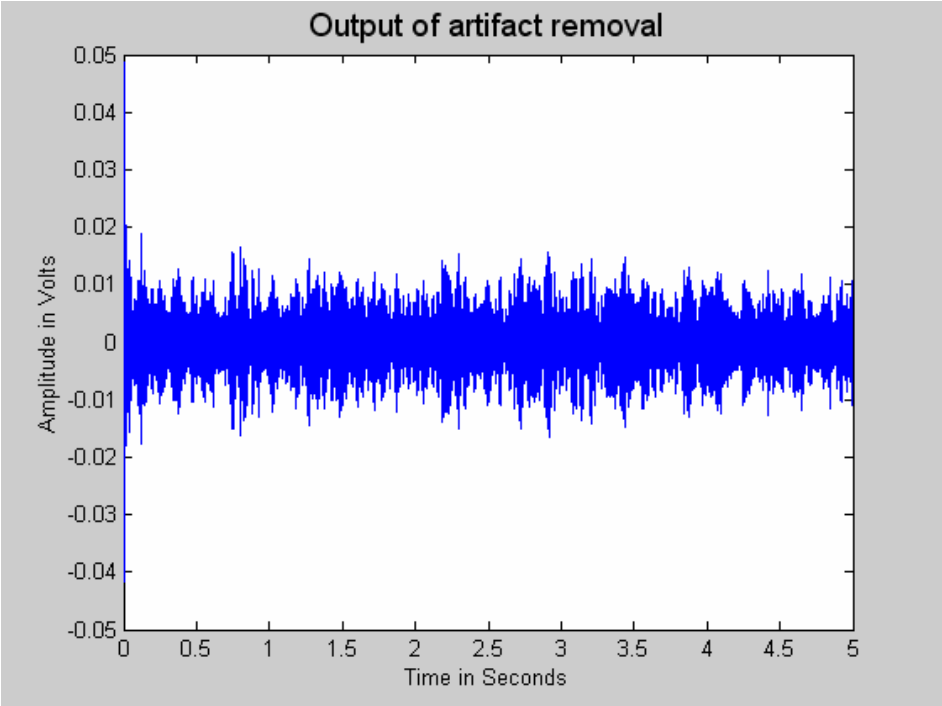

Figure 4.17: Illustration of the output of artifact removal with f_1=3000Hz

4.7 Results for frequency content of output of artifact removal

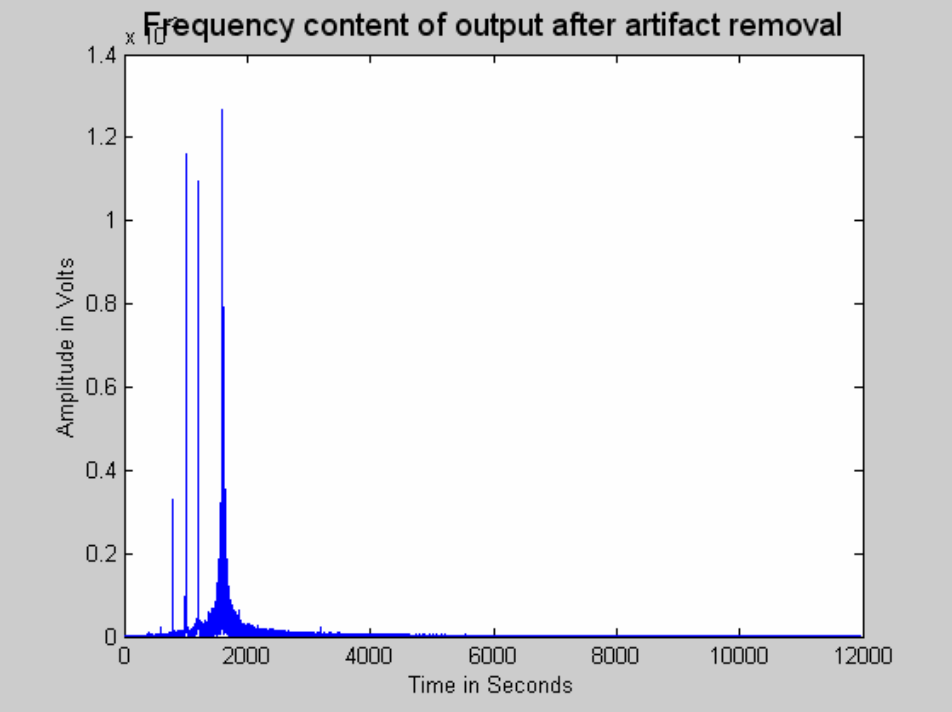

Figure 4.18: Illustration of the frequency content of output of artifact removal with f_1=1000Hz

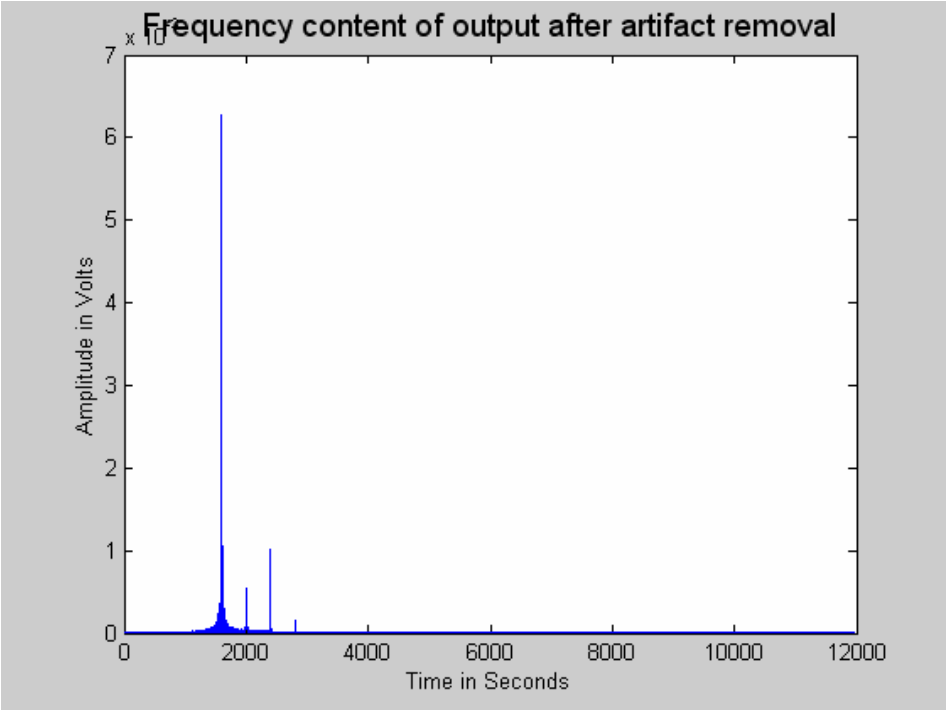

Figure 4.19: Illustration of the frequency content of output of artifact removal with f_1=2000Hz

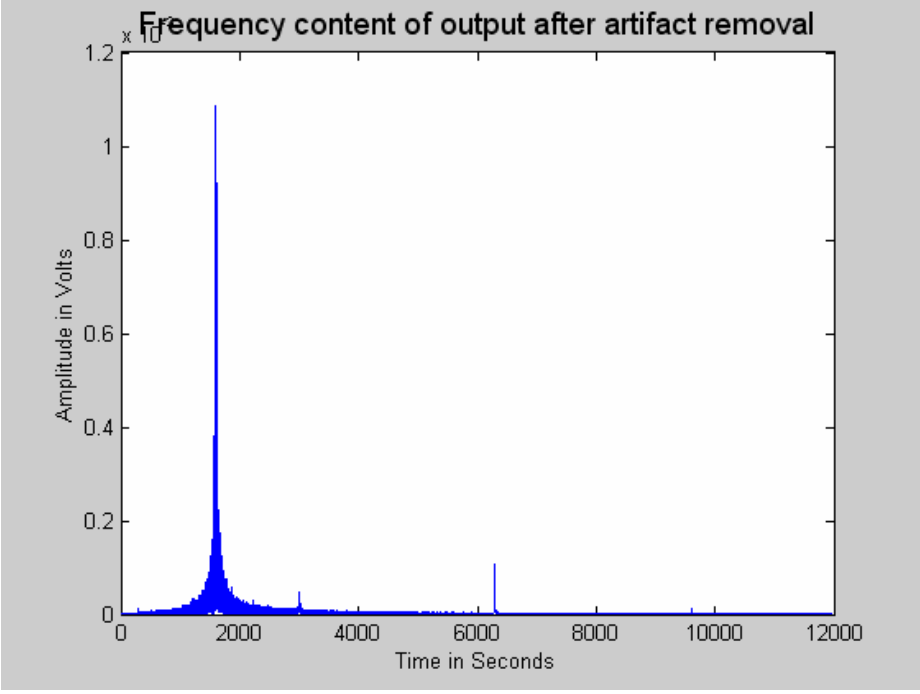

Figure 4.20: Illustration of the frequency content of output of artifact removal with f_1=3000Hz

4.8 Results for the output of mid-processing BPF

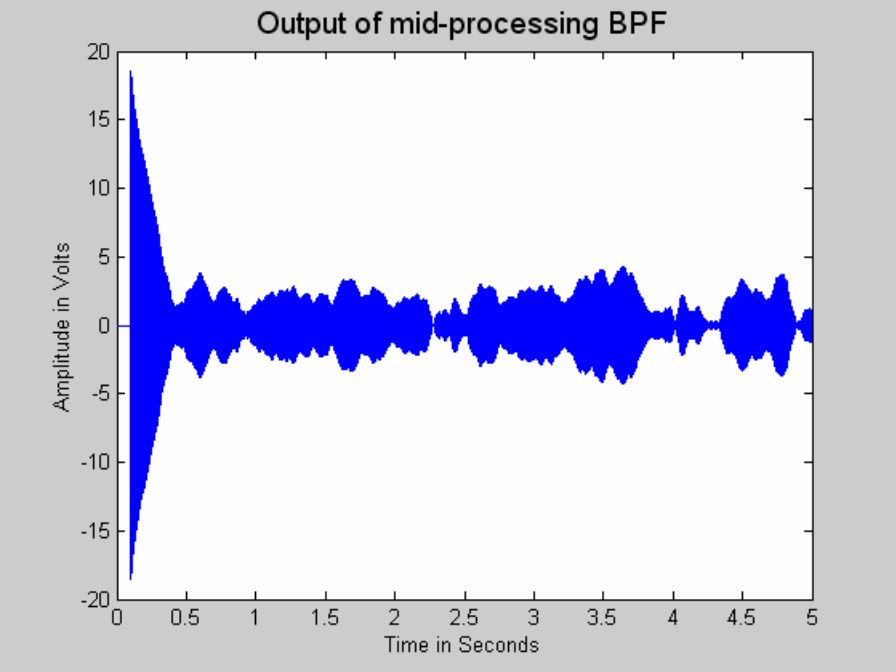

Figure 4.21: Illustration of the output of mid-processing BPF with f_1=1000Hz

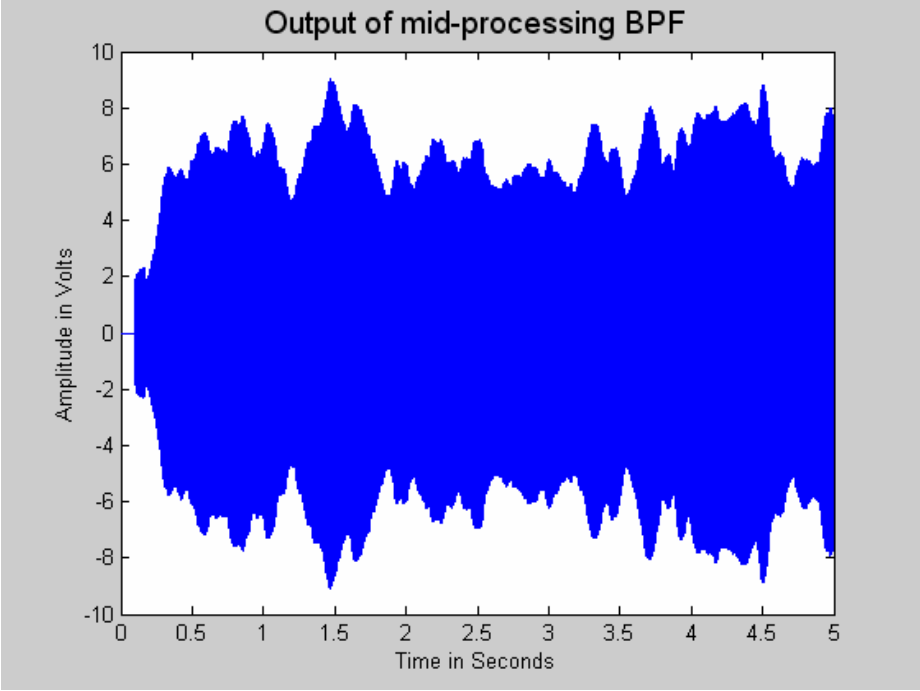

Figure 4.22: Illustration of the output of mid-processing BPF with f_1=2000Hz

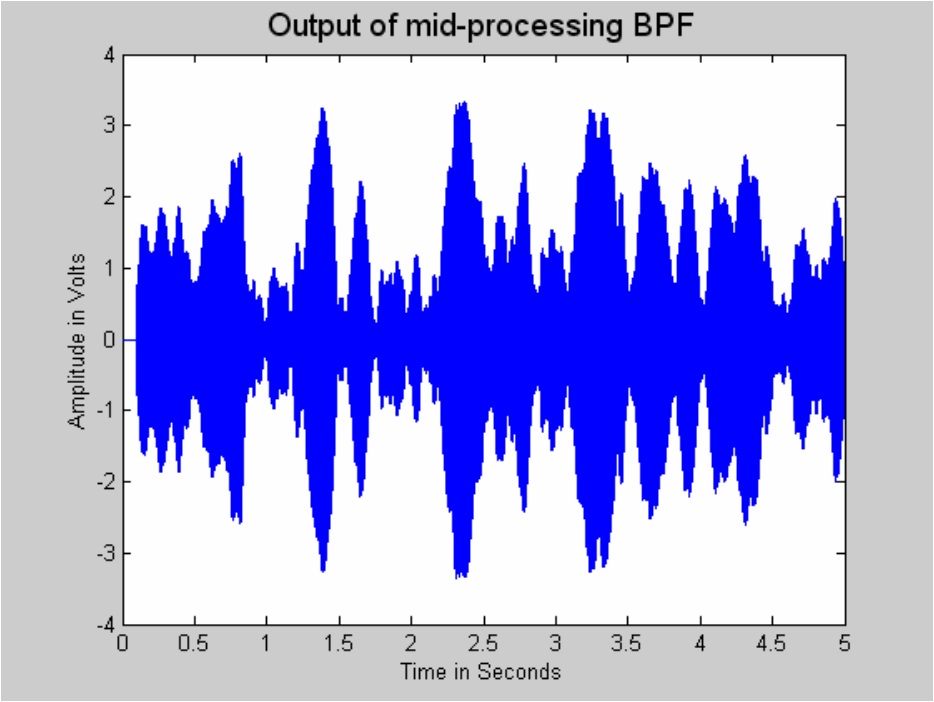

Figure 4.23: Illustration of the output of mid-processing BPF with f_1=3000Hz

4.9 Results for the frequency content of the output from mid-processing BPF

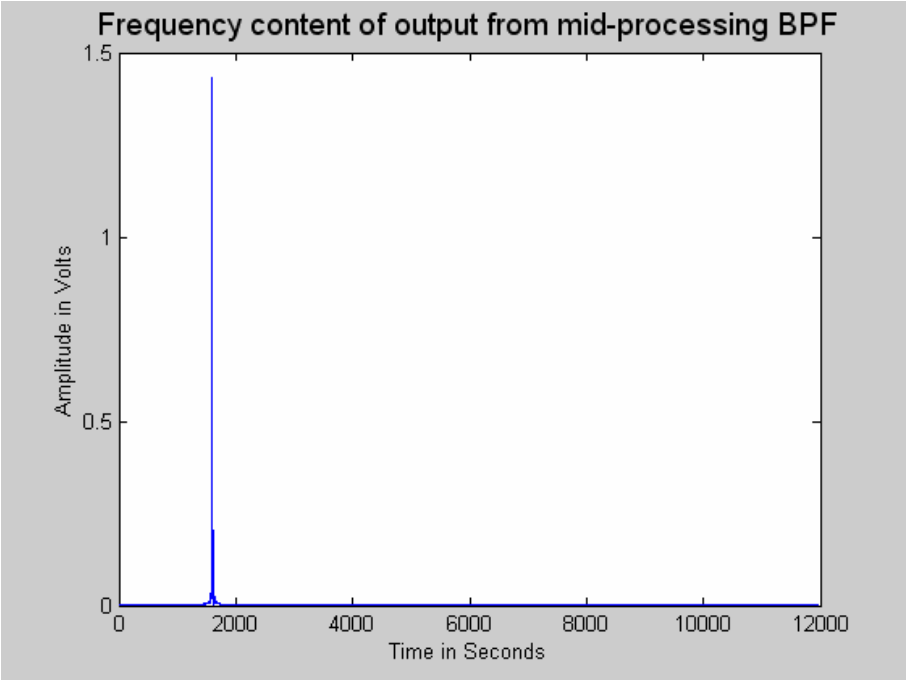

Figure 4.24: Illustration of a frequency content of the output from mid-processing BPF with f_1=1000Hz

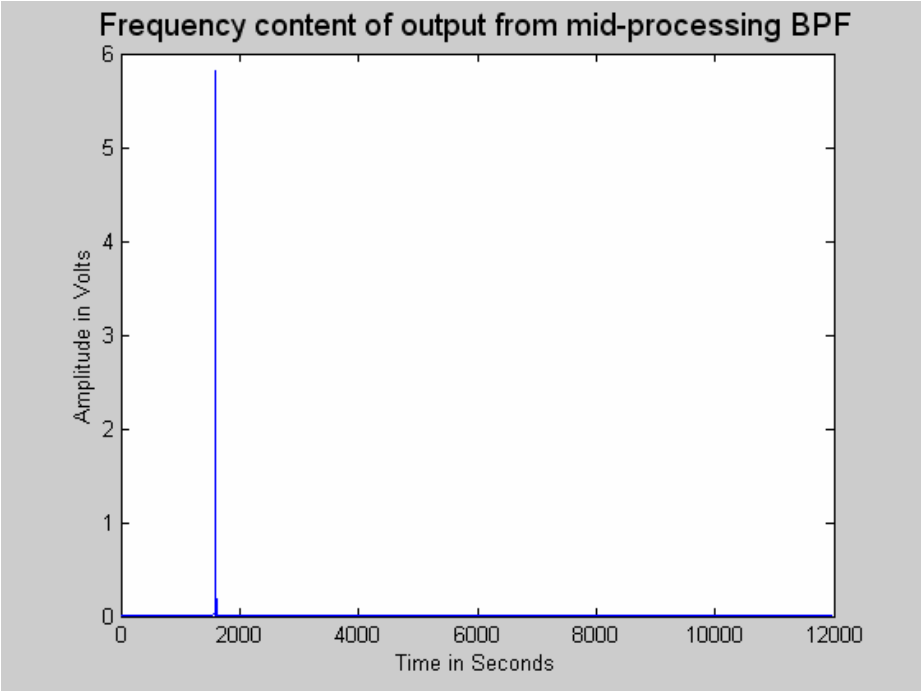

Figure 4.25: Illustration of a frequency content of the output from mid-processing BPF with f_1=2000Hz

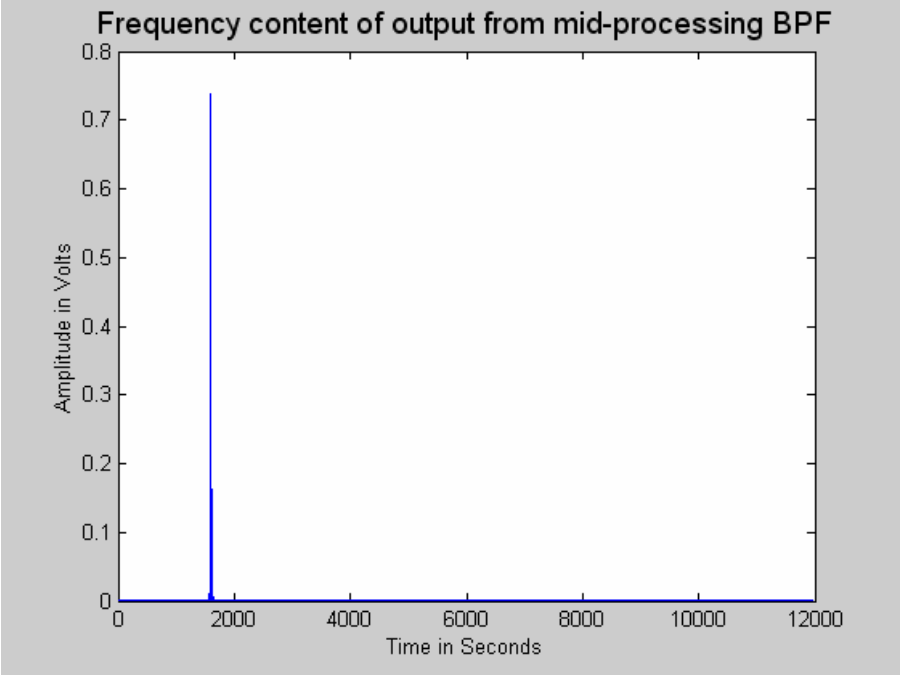

Figure 4.26: Illustration of a frequency content of the output from mid-processing BPF with f_1=3000Hz

4.10 Results for the output of DPOAE extraction

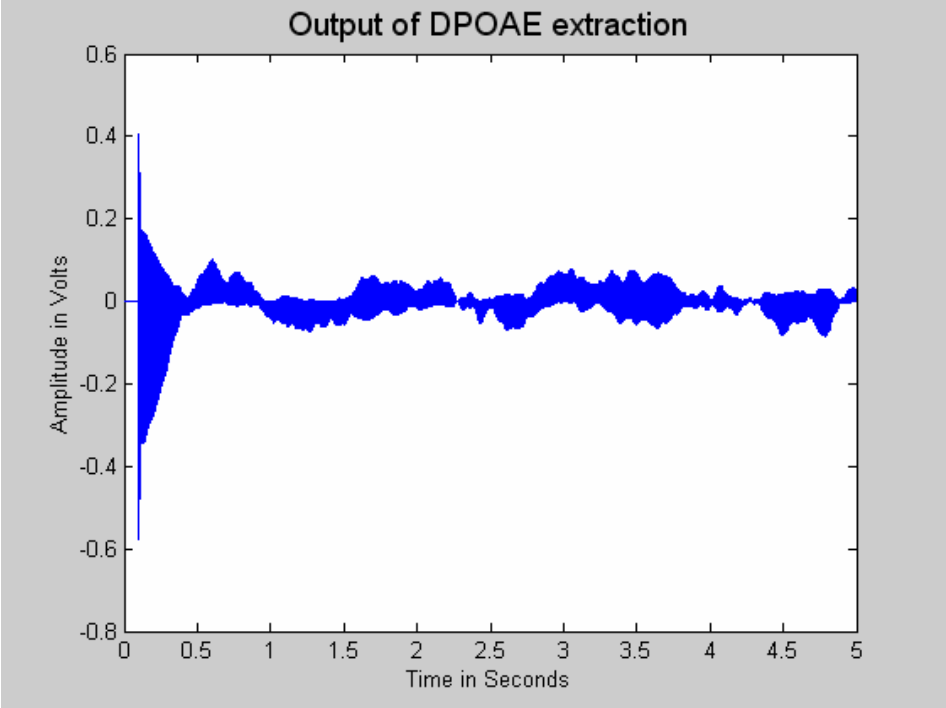

Figure 4.27: Illustration of the output of DPOAE extraction with f_1=1000Hz

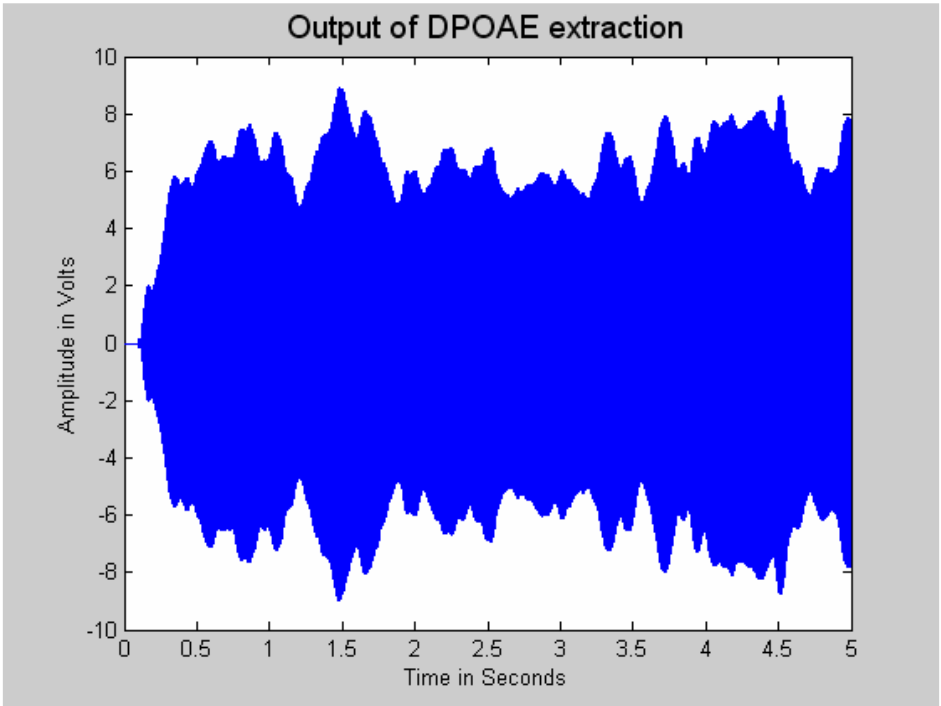

Figure 4.28: Illustration of the output of DPOAE extraction with f_1=2000Hz

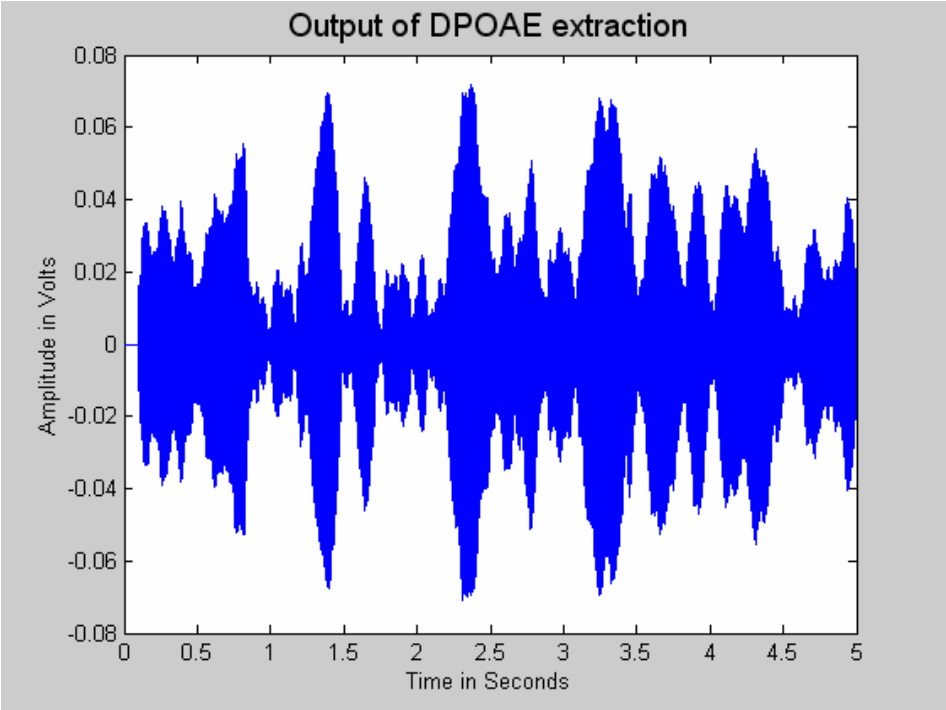

Figure 4.29: Illustration of the output of DPOAE extraction with f_1=3000Hz

4.11 Results for the frequency content of output after DPOAE extraction

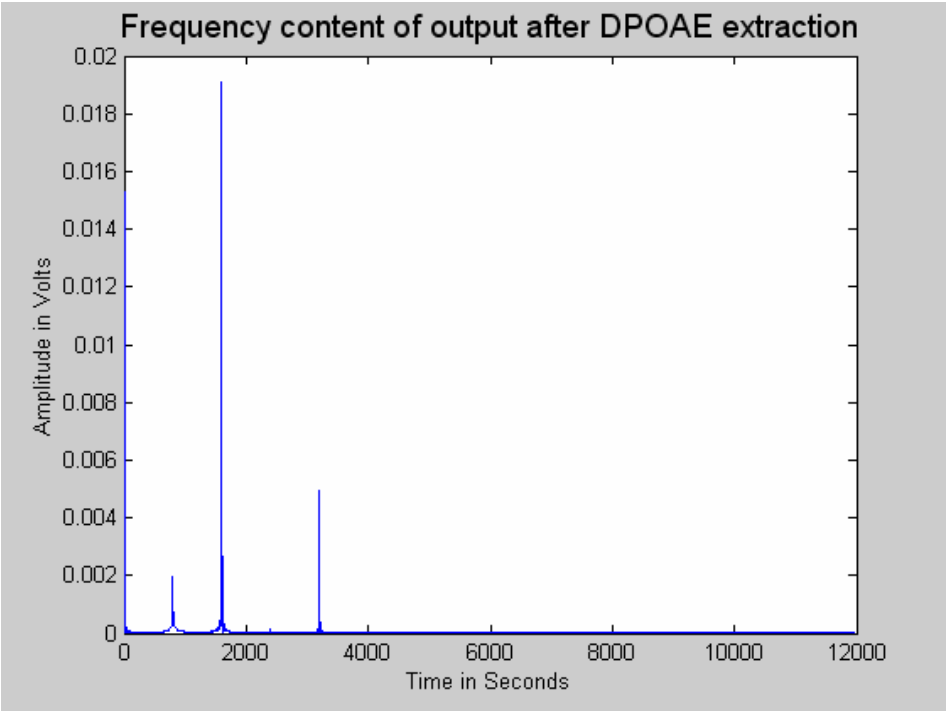

Figure 4.30: Illustration of the frequency content of output after DPOAE extraction with f_1=1000Hz

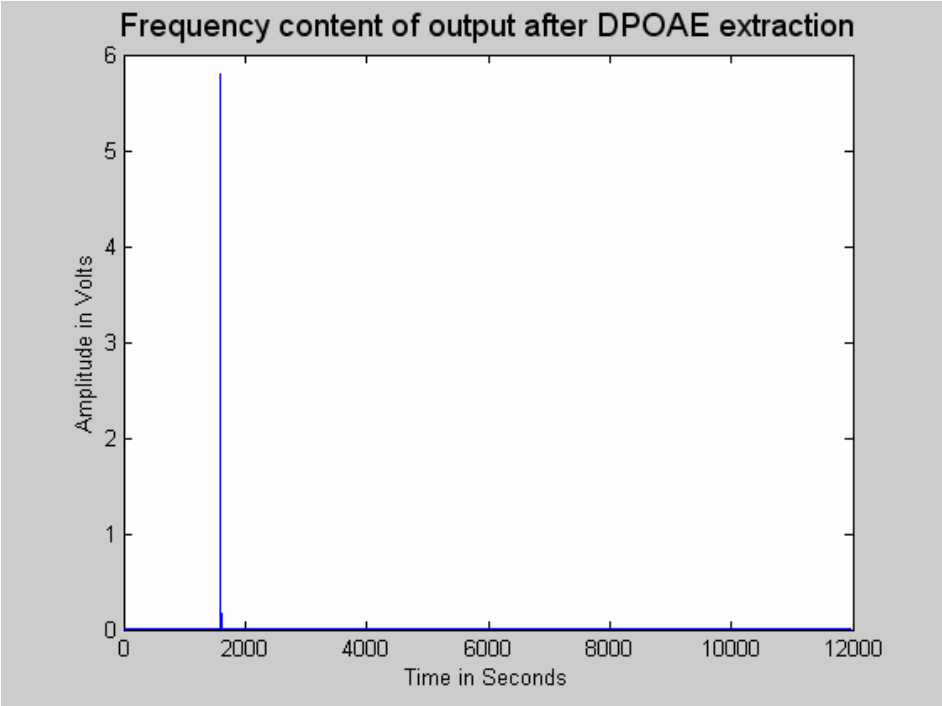

Figure 4.31: Illustration of the frequency content of output after DPOAE extraction with f_1=2000Hz

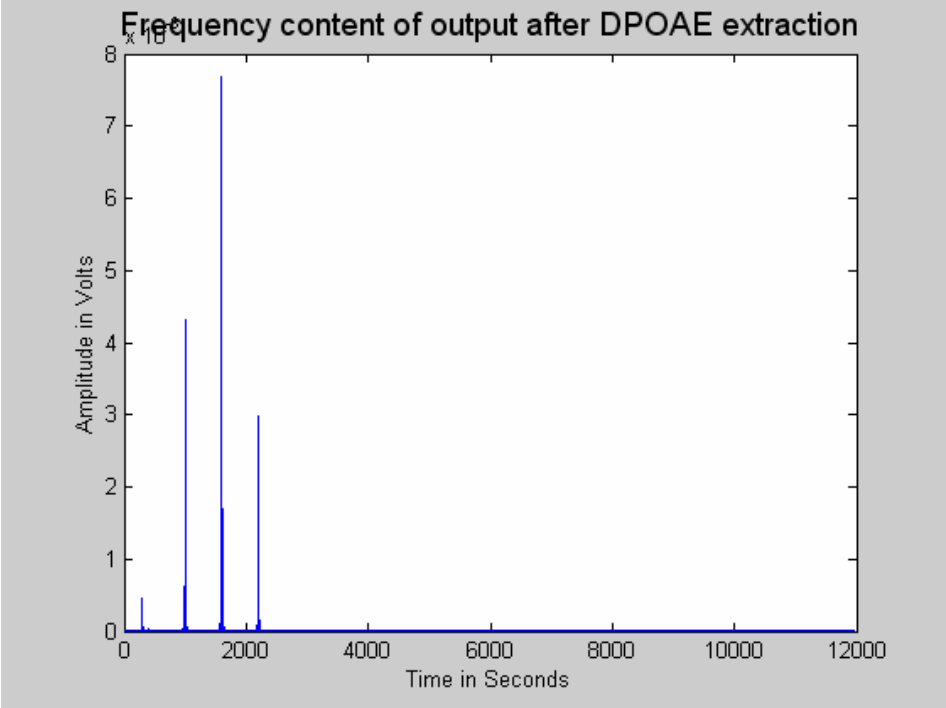

Figure 4.32: Illustration of the frequency content of output after DPOAE extraction with f_1=3000Hz

4.12 Results for DPOAE after post-processing

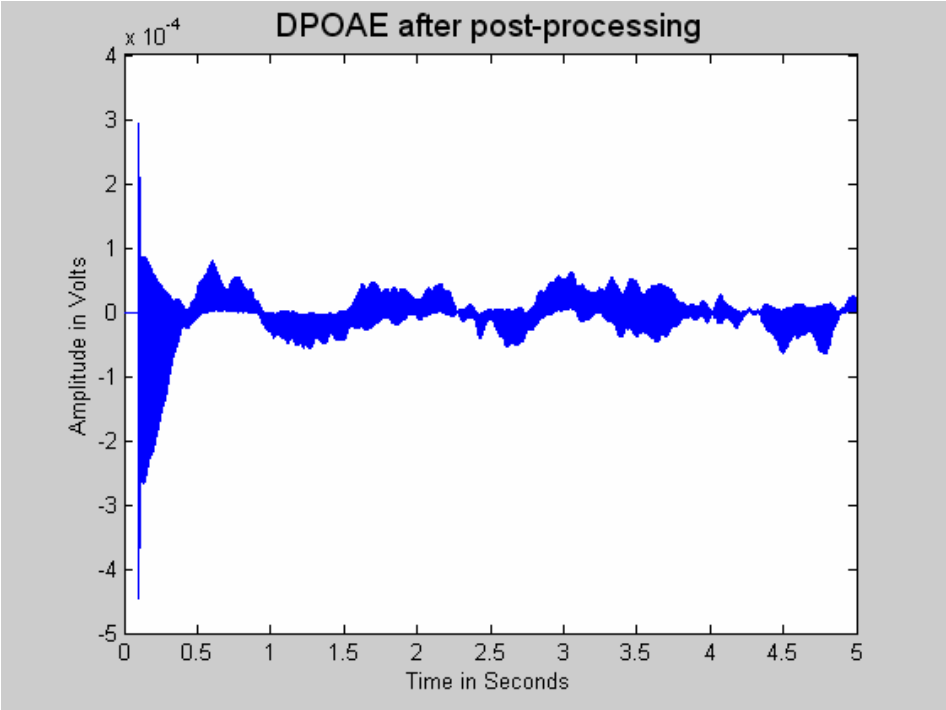

Figure 4.33: Illustration of the DPOAE after post-processing with f_1=1000Hz

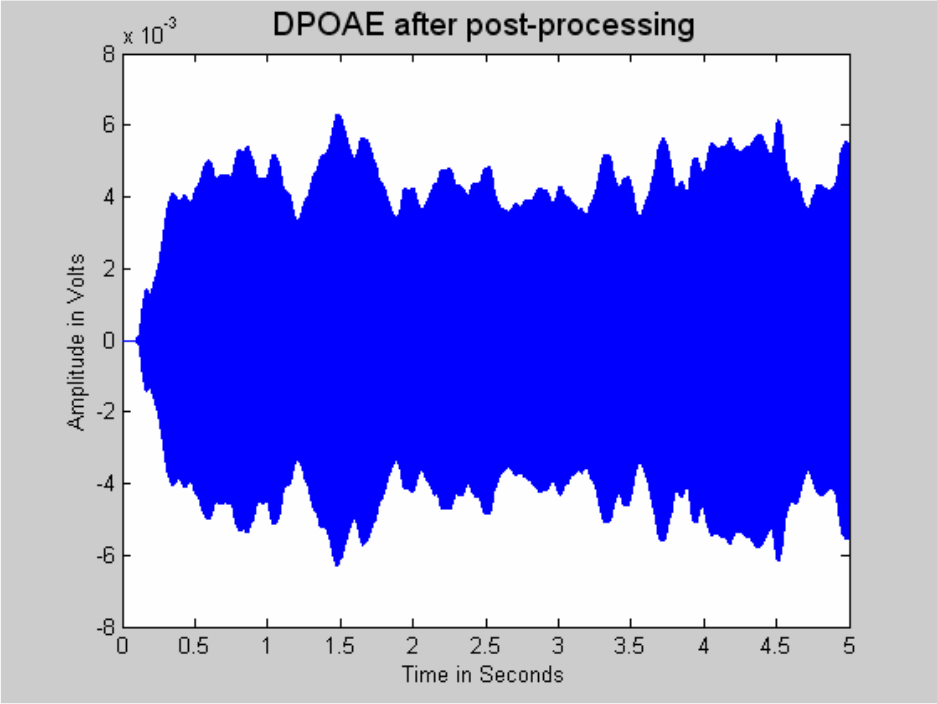

Figure 4.34: Illustration of the DPOAE after post-processing with f_1=2000Hz

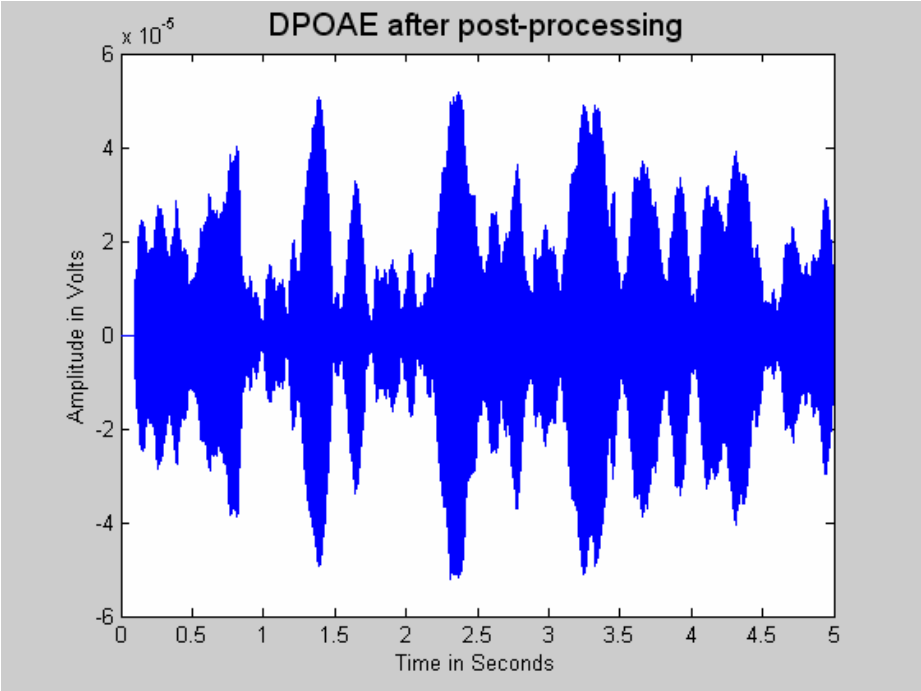

Figure 4.35: Illustration of the DPOAE after post-processing with f_1=3000Hz

4.13 Results for the frequency content DPOAE after post-processing

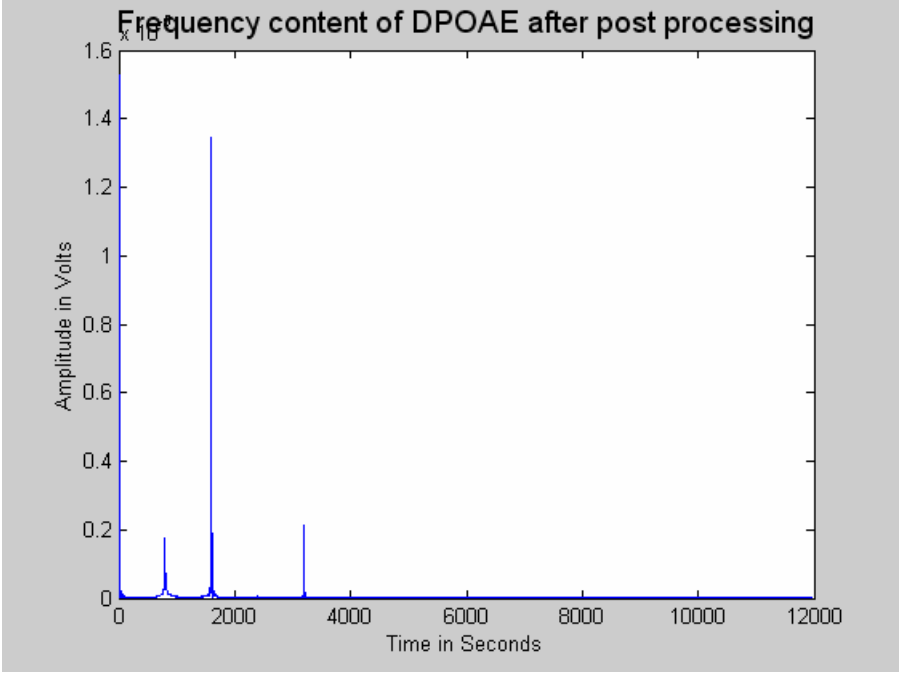

Figure 4.36: Illustration of the frequency content of DPOAE after post processing with f_1=1000Hz

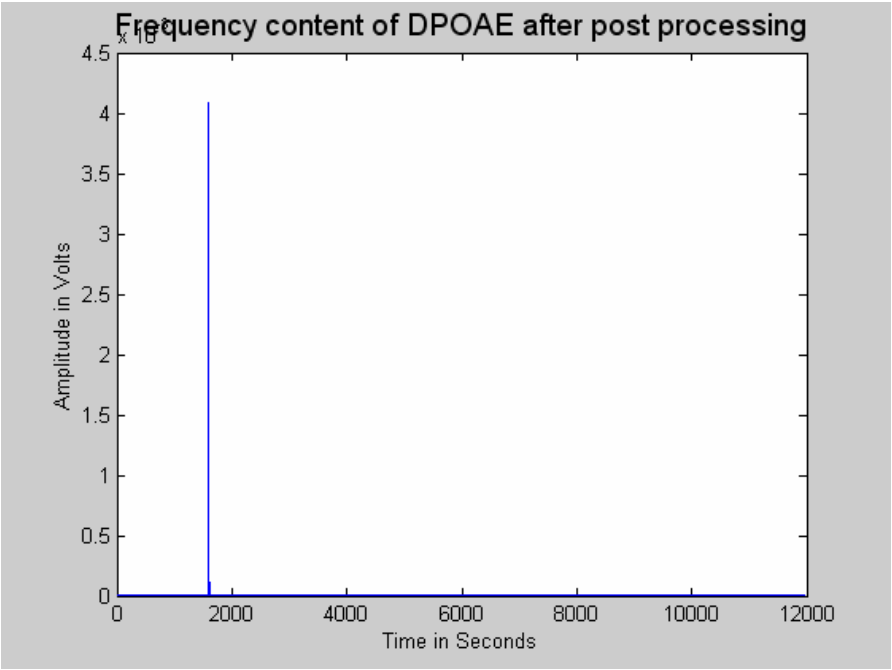

Figure 4.37: Illustration of the frequency content of DPOAE after post processing with f_1=2000Hz

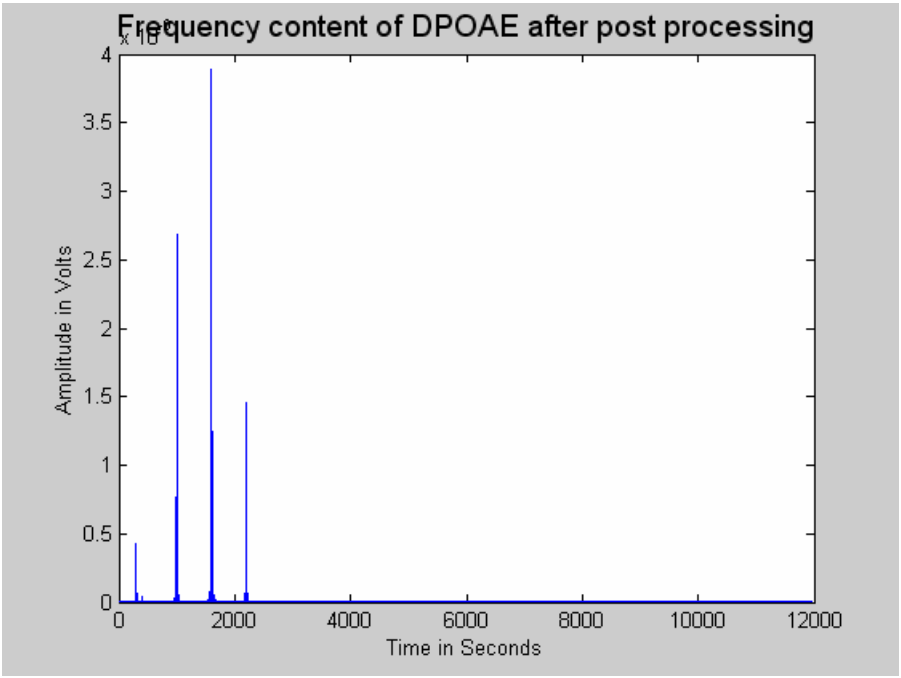

Figure 4.38: Illustration of the frequency content of DPOAE after post processing with f_1=3000Hz

4.14 Results for the DPOAE level after post-processing

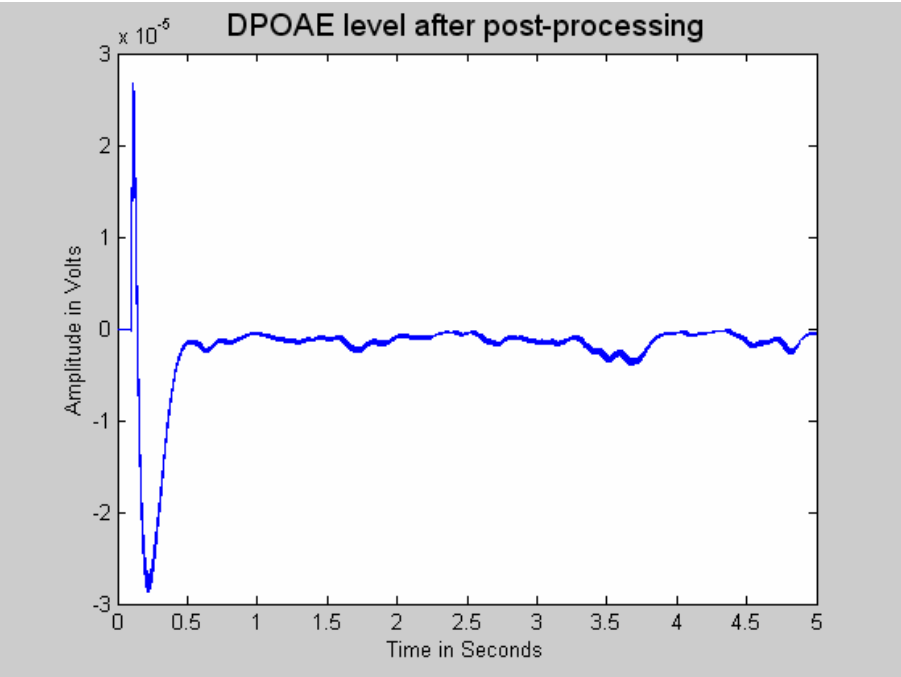

Figure 4.39: Illustration of the DPOAE level after post-processing with f_1=1000Hz

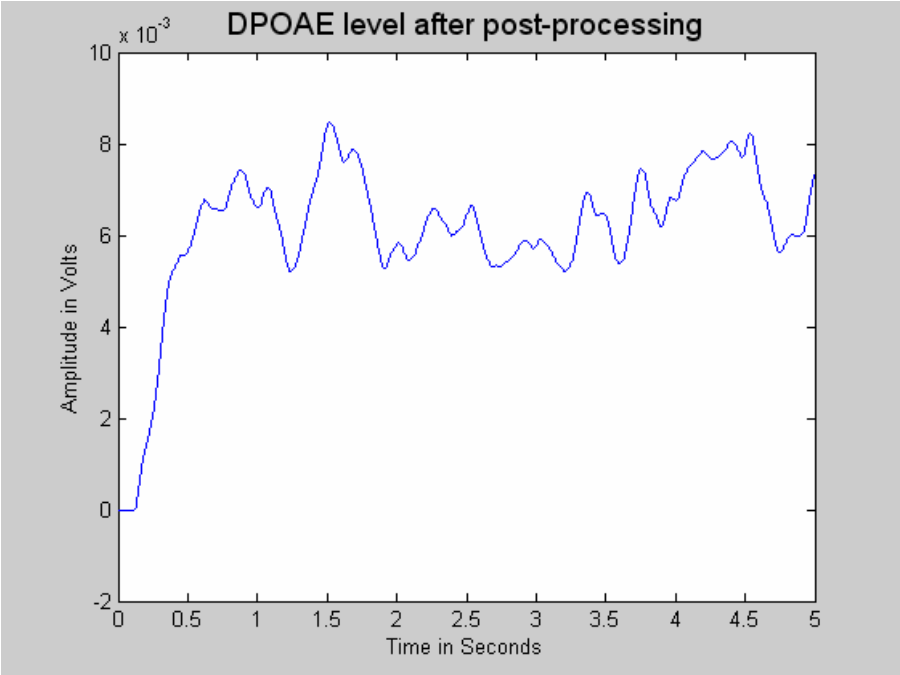

Figure 4.40: Illustration of the DPOAE level after post-processing with f_1=2000Hz

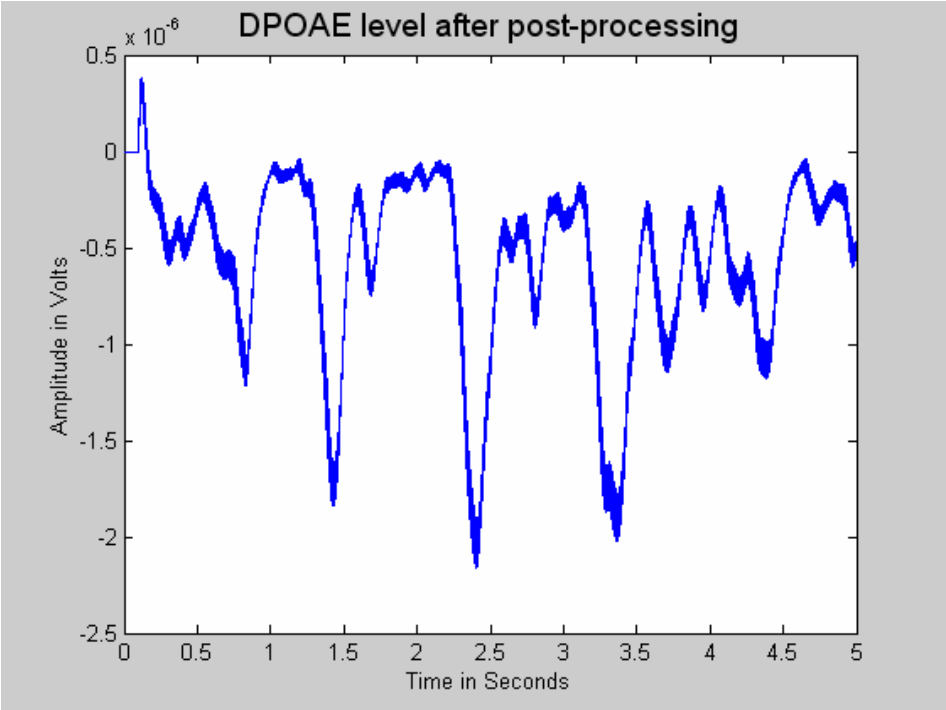

Figure 4.41: Illustration of the DPOAE level after post-processing with f_1=3000Hz

Table 4.1: Frequency Change And Random Constant Phases

F_1 in Hz	F_2 in Hz	F_D = 2*F1-F2 in Hz	delta1	delta2	deltad
1000	1200	800	2.2171	5.1093	0.0620
2000	2400	1600	2.5778	5.6150	0.3637
3000	3600	2400	2.5491	5.8777	5.7611

Table 4.2: Frequency Change And Constant Random Phase

Desired Extraction Frequency(F_D) in Hz	Constant Random Phase Delta (∂)	μ_1 and μ_2
50	1.4523	20
100	5.9698	20
150	5.1611	20
150	3.8129	200

MATLAB provides evidence of the successful implementation of the DPOAE estimation algorithm in the form of a discrete system. The noise floor was raised significantly, and the performance at each stage was obtained. In this set of plots a relatively high noise

floor of about 15 to 20 dB is introduced to the input signal (the DPOAE signal and the primaries are kept the same).

Similar results in each version of the proposed DPOAE estimation algorithm. The small differences can be attributed to the stochastic nature of the large amounts of noise present. The proposed DPOAE estimation algorithm is robust when implemented using MATLAB simulation and immune to noise.

The MATLAB implementation of the proposed DPOAE estimation technique provides a means of evaluating the real-time implementation. Doing so will allow a more modular design, and in turn, easier debugging of the real-time DSP implementation.

As observed from figure 4.39, 4.40 and 4.41,the distortion increases as f_1 is changed from 2000 Hz [f_1 is supposed to be a constant].From table 4.2, it is observed that maximum ∂ value is obtained when μ_1 and μ_2 are 20 and F_D is 100. The ∂ value decreases if the F_D value or μ_1 and μ_2 values are changed.

CHAPTER 5

CONCLUSION AND FUTURE SCOPE

CONCLUSION

A method of measurement of DPOAE signal level employing a recently introduced nonlinear adaptive signal processing technique is presented. Performance of the proposed method is demonstrated using simulations in MATLAB. Using a nonlinear adaptive algorithm as the basis for a proposed method of DPOAE estimation overcomes the shortcomings of the DFT and other linear methods. The algorithm has a high level of robustness, meaning it is extremely insensitive to changes in internal parameters and external conditions. Also, the algorithm has a high noise immunity and a relatively fast convergence speed. Combining the core algorithm with a few other signal processing units, such as band-pass and low-pass filters, allows the proposed DPOAE estimation process to quickly and accurately estimate DPOAE signals in noisy environments.

As already stated, the main features of the proposed method of DPOAE signal measurement are its 1) structural simplicity, 2) high noise immunity and robustness, and 3) relatively high speed of convergence. Given the low complexity of the proposed method, it requires low level of computational resources, which in turn translates into less expensive equipment. High noise immunity and robustness of the proposed method render it suitable for practical applications. High speed of convergence of the proposed method is useful in reducing the time taken to perform the test.

FUTURE SCOPE

DPOAE estimation simulation has been done. The hardware implementation of this can be carried out. The comparison of the software simulations presented and the hardware results can be done.

REFERENCES

[1] R. E. Delgado, O. Ozdamar, S. Rahman, and C. N. Lopez, “Adaptive noise cancellation in a multimicrophone system for distortion product otoacoustic emission acquisition,” *IEEE Trans. Biomed. Eng.*, vol. 47, Sept. 2000.

[2] D. T. Kemp, “Stimulated acoustic emissions from within the human auditory system,” *J. Acoust. Soc. Amer.*, vol. 64, 1978.

[3] R. Probst, B. L. Lonsbury-Martin, and G. K. Martin, “A review of otoacoustic emissions,” *J. Acoust. Soc. Amer.*, vol. 89, 1991.

[4] X. Li, Y. Sokolov, and H. Kunov, “System and method for processing lowsignal-to-noise ratio signals,” May 18, 2000.

[5] M. Karimi-Ghartemani and A. K. Ziarani, “Periodic orbit analysis of two dynamical systems for electrical engineering applications,” *J. Eng. Math.*, vol. 45, 2003.

[6] A. K. Ziarani and A. Konrad, “A nonlinear adaptive method of elimination of power line interference in ECG signals,” *IEEE Trans. Biomed. Eng.*, vol. 49, June 2002.

[7] A. K. Ziarani, A. Konrad, and A. N. Sinclair, “A novel time-domain method of analysis of pulsed sine wave signals,” *IEEE Trans. Instrum. Meas.*, Mar. 2003.

[8] W. K. Ma and Y. T. Zhang, “Estimation of distortion product otoacoustic emissions,” *IEEE Trans. Biomed. Eng.*, vol. 46, Oct.1999.

[9] P. F. Craigmile and W. M. King, “Periodogram based tests for distortion product otoacoustic emissions," *The Journal of the Acoustical Society of America,* Vol. 116, 2004.

[10] Web site of the Cincinnati Children's Hospital Medical Center, “Hearing tests," 2004, http://www.cincinnatichildrens.org/health/info/ent/procedure/hearing-tests.htm.

[11] B. A. Prieve, T. S. Fitzgerald, L. A. Schultze, and D. T. Kemp, “Basic characteristics of distortion product otoacoustic emissions in infants and children," *The Journal of the Acoustical Society of America,* Vol. 102, 1997.

[12] A. K. Ziarani and A. Konrad, “A novel method of estimation of DPOAE signals," *IEEE Transactions on Biomedical Engineering,* Vo. 51, 2004.

[13] R. E. Delgado, O. Ozdamar, S. Rahman, and C. N. Lopez, “Adaptive noise cancellation in a multimicrophone system for distortion product otoacoustic emission acquisition," *IEEE Transactions on Biomedical Engineering,* Vol. 47, 2000.

[14] Web site of Southern Arkansas University - Magnolia, General Psychology webpage, http://peace.saumag.edu/faculty/Kardas/Courses/GPWeiten/C4SandP/Ear.JPG.

[15] Web site of Indiana University - Bloomington, Department of Physical webpage, http://physics.indiana.edu/ p105 f02/cochlea.gif.

[16] L. Bian, E. E. Linhardt, and M. E. Chertoff, “Cochlear hysteresis: observation with low-frequency modulated distortion product otoacoustic emissions," *The Journal of the Acoustical Society of America,* Vol. 115, 2004.

[17] E. Gonzalo, D. V. Llanes, and C. M. Chiong, “Evoked otoacoustic emiassions and auditory brainstem responses: concordance in hearing screening among high-risk children,"*Acta Oto-Laryngologica,* Vol. 1234, 2004.

[18] Website of the Otoacoustic Emissions Portal Zone, “Spontaneous otoacoustic emissions," September 2004, http://www.otoemissions.org/index 1024.html.

[19] W. K Ma and Y. T. Zhang, “Estimation of distortion product otoacoustic emissions," *IEEE Transactions on Biomedical Engineering,* Vol. 46, 1999.

[20] J. Muller and T. Janssen, “Similarity in loudness and distortion product otoacoustic emission input/output functions: implications for an objective hearing aid adjustment," *The Journal of the Acoustical Society of America,* Vol. 115, 2004.

[21] B. Davis, W. Qiu, and R. P. Hamernik, “The use of distortion product otoacoustic emissions ni the estimation of hearing and sensory cell loss in noise-damaged cochleas," *Hearing Research,* Vol. 187, 2004.

[22] T. Janssen, P. Kummer, and W. Arnold, “Growth behavior of the $2f_1 - f_2$ distortion product otoacoustic emission in tinnitus," *The Journal of the Acoustical Society of America,* Vol. 103, 1998.

[23] A. Nevchihan, A. Ferda, and U. Yekta, “Detection of sensorineural hearing impairment by using DPOAE technique and classifiers," *Proceedings of the IEEE* 17th *Annual Engineering in Medicine and Biology Conference,* Montreal, Canada, Vol. 2, September, 1995.

[24] A. N Lukashkin and I. J. Russell, “Origin of the bell-like dependence of the DPOAE

amplitude on primary frequency ratio," *The Journal of the Acoustical Society of America,* Vol. 110, 2001.

[25] A. N. Lukashkin and I. J. Russell, “Modification of a single saturating non-linearity for post-onset changes ni 2 $f_1 - f_2$ distortion product otoacoustic emission," *The Journal of the Acoustical Society of America,* Vol. 112, 2002

LIST OF PUBLICATIONS

- Submitted a paper on "**MEDICAL IMAGING APPLICATIONS-DSP SOLUTION USING FPGA"** in national conference on **ELECTRONIC CIRCUITS AND COMMUNICATION SYSTEMS** at THAPAR INSTITUTE OF ENGG. & TECH., PATIALA in February 2006.

- Submitted a paper on "**VARIABLE SPEED CONTROL OF AC MACHINES USING DSP"** in national conference on **ELECTRONIC CIRCUITS AND COMMUNICATION SYSTEMS** at THAPAR INSTITUTE OF ENGG. & TECH., PATIALA in February 2006.